

DOCUMENTATION PAGE				FILE COPY
AD-A214 110				1b. RESTRICTIVE MARKINGS
07 1989				3. DISTRIBUTION/AVAILABILITY OF REPORT Approved for public release; distribution unlimited.
4. PERFORMING ORGANIZATION REPORT NUMBER(S)				5. MONITORING ORGANIZATION REPORT NUMBER(S) ARO 23233.10-PH
6a. NAME OF PERFORMING ORGANIZATION IBM Research, Yorktown		6b. OFFICE SYMBOL (if applicable)		7a. NAME OF MONITORING ORGANIZATION U. S. Army Research Office
6c. ADDRESS (City, State, and ZIP Code) P.O. Box 218 Yorktown Heights, NY 10598		7b. ADDRESS (City, State, and ZIP Code) P. O. Box 12211 Research Triangle Park, NC 27709-2211		
8a. NAME OF FUNDING/SPONSORING ORGANIZATION U. S. Army Research Office		8b. OFFICE SYMBOL (if applicable)		9. PROCUREMENT INSTRUMENT IDENTIFICATION NUMBER DAAL03-86-K-0008
8c. ADDRESS (City, State, and ZIP Code) P. O. Box 12211 Research Triangle Park, NC 27709-2211		10. SOURCE OF FUNDING NUMBERS PROGRAM ELEMENT NO. PROJECT NO. TASK NO. WORK UNIT ACCESSION NO.		
11. TITLE (Include Security Classification) Sub-Picosecond Laser Studies of Excited State Dynamics				
12. PERSONAL AUTHOR(S) J. H. Glowina, J. Misewich and P. P. Sorokin				
13a. TYPE OF REPORT Final		13b. TIME COVERED FROM 8/86 TO 8/89		14. DATE OF REPORT (Year, Month, Day) 1989, October
15. PAGE COUNT 21 plus figures				
16. SUPPLEMENTARY NOTATION The view, opinions and/or findings contained in this report are those of the author(s) and should not be construed as an official Department of the Army position, policy, or decision, unless so designated by other documentation.				
17. COSATI CODES FIELD GROUP SUB-GROUP			18. SUBJECT TERMS (Continue on reverse if necessary and identify by block number) Amplification of femtosecond UV beams in excimers, gas-phase continuum generation, transition-state spectroscopy of Tl, Bi, Na and CN, internal conversion in DABCO.	
19. ABSTRACT (Continue on reverse if necessary and identify by block number) Under contract DAAL03-86-C-0008, apparatus for performing femtosecond transition-state absorption spectroscopy has been developed. The UV pump pulses rely upon amplification of femtosecond pulses in excimers. The probe pulses rely upon gas-phase continuum generation. Both effects were first realized and/or discovered by our group during the contract period just completed. <i>(Thallium, Sodium Bismuth)</i> With the above apparatus, femtosecond transition-state absorption spectroscopy has been performed on Tl, Na and Bi atoms produced by the 308-nm and 248-nm photodissociation of various gas-phase molecules, and also on CN radicals produced by UV photolysis of ICN. In the case of Tl and Bi, the transient spectra are all clearly identifiable as atomic, yet they display striking asymmetries in line shapes and enhancements in intensity that clearly demonstrate that they are spectral signatures of atoms still in the force fields of their receding partners. A new area of spectroscopy has thus been defined. <i>Yes, it is a new area of spectroscopy.</i>				
20. DISTRIBUTION/AVAILABILITY OF ABSTRACT <input type="checkbox"/> UNCLASSIFIED/UNLIMITED <input type="checkbox"/> SAME AS RPT. <input type="checkbox"/> DTIC USERS			21. ABSTRACT SECURITY CLASSIFICATION Unclassified	
22a. NAME OF RESPONSIBLE INDIVIDUAL			22b. TELEPHONE (Include Area Code)	22c. OFFICE SYMBOL

**Sub-Picosecond Laser Studies of Excited State Dynamics**

**FINAL REPORT**

**P.P. Sorokin, J.H. Glowina, and J.A. Misewich**

**Oct. 6, 1989**

**U.S. Army Research Office**

**DAAL03-86-C-0008**

**IBM Thomas J. Watson Research Center**

**Yorktown Heights, New York, 10598**

**APPROVED FOR PUBLIC RELEASE**

**DISTRIBUTION UNLIMITED**

The view, opinions, and/or findings contained in this report are those of the authors and should not be construed as an official Department of the Army position, policy, or decision, unless so designated by other documentation.

## 1. Introduction

Several objectives outlined in the original technical proposal (see IBM Technical Proposal: Sub-Picosecond Laser Studies of Excited-State Dynamics ) were fulfilled in the work done under the just completed three-year contract (1 Aug 1986- 31 July 1989). A comparison of results that were actually achieved with our stated goals serves as the loosely-defined structure for this final report. Results are presented approximately in the order they were obtained.

## 2. Amplification of Femtosecond Pulses in Excimer Gain Modules

The main thrust of our original proposal was contained in Sec. II of that proposal, entitled "Subpicosecond Broadband Absorption Spectroscopy of Photodissociating Molecules". It was there proposed that, through developments in ultrafast light pulse technology, it might be possible "to record the spectra of molecules actually in the process of photodissociation and of fragments actually in the process of being formed." To achieve this goal appeared to require development of a powerful femtosecond UV photolytic source. Amplification of femtosecond pulses in excimer gain modules was identified, in turn, as the most promising means to realize the latter, although, at the time, subpicosecond pulse amplification in excimers had not yet been reported.

We began our (DAAI.03-86-C-0008) contract work, focussing on the development of a subpicosecond photolytic source, one based upon amplification in XeCl gain modules. Seed pulses for the excimer amplifier were formed through the use of a synch-pumped mode-locked dye laser tuned to 616 nm, a single-mode fiber pulse compressor, a four-stage Nd<sup>3+</sup>:YAG-laser-pumped dye amplifier, and finally, a KDP frequency doubling crystal. A pair of XeCl gain modules was used to amplify the 350-fsec seed pulses to ~10-mJ energies with ~ 1-mJ amplified spontaneous emission content. The publication<sup>1</sup> describing this result was the *first published account of subpicosecond laser pulse amplification in excimer gain modules*. The optical layout of the apparatus finally realized was quite similar to the proposed layout shown in Fig. 2 of our original technical proposal. (Only, we overestimated the maximum short-pulse output energy by roughly a factor 5, as we proposed use of double-pass amplification in one of the two XeCl amplifiers, which we now know to be unrealistic in view of the ASE that would be generated.)

1  
2  
3  
4  
5  
6  
7  
8  
9  
10  
11  
12  
13  
14  
15  
16  
17  
18  
19  
20  
21  
22  
23  
24  
25  
26  
27  
28  
29  
30  
31  
32  
33  
34  
35  
36  
37  
38  
39  
40  
41  
42  
43  
44  
45  
46  
47  
48  
49  
50  
51  
52  
53  
54  
55  
56  
57  
58  
59  
60  
61  
62  
63  
64  
65  
66  
67  
68  
69  
70  
71  
72  
73  
74  
75  
76  
77  
78  
79  
80  
81  
82  
83  
84  
85  
86  
87  
88  
89  
90  
91  
92  
93  
94  
95  
96  
97  
98  
99  
100  
101  
102  
103  
104  
105  
106  
107  
108  
109  
110  
111  
112  
113  
114  
115  
116  
117  
118  
119  
120  
121  
122  
123  
124  
125  
126  
127  
128  
129  
130  
131  
132  
133  
134  
135  
136  
137  
138  
139  
140  
141  
142  
143  
144  
145  
146  
147  
148  
149  
150  
151  
152  
153  
154  
155  
156  
157  
158  
159  
160  
161  
162  
163  
164  
165  
166  
167  
168  
169  
170  
171  
172  
173  
174  
175  
176  
177  
178  
179  
180  
181  
182  
183  
184  
185  
186  
187  
188  
189  
190  
191  
192  
193  
194  
195  
196  
197  
198  
199  
200  
201  
202  
203  
204  
205  
206  
207  
208  
209  
210  
211  
212  
213  
214  
215  
216  
217  
218  
219  
220  
221  
222  
223  
224  
225  
226  
227  
228  
229  
230  
231  
232  
233  
234  
235  
236  
237  
238  
239  
240  
241  
242  
243  
244  
245  
246  
247  
248  
249  
250  
251  
252  
253  
254  
255  
256  
257  
258  
259  
260  
261  
262  
263  
264  
265  
266  
267  
268  
269  
270  
271  
272  
273  
274  
275  
276  
277  
278  
279  
280  
281  
282  
283  
284  
285  
286  
287  
288  
289  
290  
291  
292  
293  
294  
295  
296  
297  
298  
299  
300  
301  
302  
303  
304  
305  
306  
307  
308  
309  
310  
311  
312  
313  
314  
315  
316  
317  
318  
319  
320  
321  
322  
323  
324  
325  
326  
327  
328  
329  
330  
331  
332  
333  
334  
335  
336  
337  
338  
339  
340  
341  
342  
343  
344  
345  
346  
347  
348  
349  
350  
351  
352  
353  
354  
355  
356  
357  
358  
359  
360  
361  
362  
363  
364  
365  
366  
367  
368  
369  
370  
371  
372  
373  
374  
375  
376  
377  
378  
379  
380  
381  
382  
383  
384  
385  
386  
387  
388  
389  
390  
391  
392  
393  
394  
395  
396  
397  
398  
399  
400  
401  
402  
403  
404  
405  
406  
407  
408  
409  
410  
411  
412  
413  
414  
415  
416  
417  
418  
419  
420  
421  
422  
423  
424  
425  
426  
427  
428  
429  
430  
431  
432  
433  
434  
435  
436  
437  
438  
439  
440  
441  
442  
443  
444  
445  
446  
447  
448  
449  
450  
451  
452  
453  
454  
455  
456  
457  
458  
459  
460  
461  
462  
463  
464  
465  
466  
467  
468  
469  
470  
471  
472  
473  
474  
475  
476  
477  
478  
479  
480  
481  
482  
483  
484  
485  
486  
487  
488  
489  
490  
491  
492  
493  
494  
495  
496  
497  
498  
499  
500  
501  
502  
503  
504  
505  
506  
507  
508  
509  
510  
511  
512  
513  
514  
515  
516  
517  
518  
519  
520  
521  
522  
523  
524  
525  
526  
527  
528  
529  
530  
531  
532  
533  
534  
535  
536  
537  
538  
539  
540  
541  
542  
543  
544  
545  
546  
547  
548  
549  
550  
551  
552  
553  
554  
555  
556  
557  
558  
559  
560  
561  
562  
563  
564  
565  
566  
567  
568  
569  
570  
571  
572  
573  
574  
575  
576  
577  
578  
579  
580  
581  
582  
583  
584  
585  
586  
587  
588  
589  
590  
591  
592  
593  
594  
595  
596  
597  
598  
599  
600  
601  
602  
603  
604  
605  
606  
607  
608  
609  
610  
611  
612  
613  
614  
615  
616  
617  
618  
619  
620  
621  
622  
623  
624  
625  
626  
627  
628  
629  
630  
631  
632  
633  
634  
635  
636  
637  
638  
639  
640  
641  
642  
643  
644  
645  
646  
647  
648  
649  
650  
651  
652  
653  
654  
655  
656  
657  
658  
659  
660  
661  
662  
663  
664  
665  
666  
667  
668  
669  
670  
671  
672  
673  
674  
675  
676  
677  
678  
679  
680  
681  
682  
683  
684  
685  
686  
687  
688  
689  
690  
691  
692  
693  
694  
695  
696  
697  
698  
699  
700  
701  
702  
703  
704  
705  
706  
707  
708  
709  
710  
711  
712  
713  
714  
715  
716  
717  
718  
719  
720  
721  
722  
723  
724  
725  
726  
727  
728  
729  
730  
731  
732  
733  
734  
735  
736  
737  
738  
739  
740  
741  
742  
743  
744  
745  
746  
747  
748  
749  
750  
751  
752  
753  
754  
755  
756  
757  
758  
759  
760  
761  
762  
763  
764  
765  
766  
767  
768  
769  
770  
771  
772  
773  
774  
775  
776  
777  
778  
779  
780  
781  
782  
783  
784  
785  
786  
787  
788  
789  
790  
791  
792  
793  
794  
795  
796  
797  
798  
799  
800  
801  
802  
803  
804  
805  
806  
807  
808  
809  
810  
811  
812  
813  
814  
815  
816  
817  
818  
819  
820  
821  
822  
823  
824  
825  
826  
827  
828  
829  
830  
831  
832  
833  
834  
835  
836  
837  
838  
839  
840  
841  
842  
843  
844  
845  
846  
847  
848  
849  
850  
851  
852  
853  
854  
855  
856  
857  
858  
859  
860  
861  
862  
863  
864  
865  
866  
867  
868  
869  
870  
871  
872  
873  
874  
875  
876  
877  
878  
879  
880  
881  
882  
883  
884  
885  
886  
887  
888  
889  
890  
891  
892  
893  
894  
895  
896  
897  
898  
899  
900  
901  
902  
903  
904  
905  
906  
907  
908  
909  
910  
911  
912  
913  
914  
915  
916  
917  
918  
919  
920  
921  
922  
923  
924  
925  
926  
927  
928  
929  
930  
931  
932  
933  
934  
935  
936  
937  
938  
939  
940  
941  
942  
943  
944  
945  
946  
947  
948  
949  
950  
951  
952  
953  
954  
955  
956  
957  
958  
959  
960  
961  
962  
963  
964  
965  
966  
967  
968  
969  
970  
971  
972  
973  
974  
975  
976  
977  
978  
979  
980  
981  
982  
983  
984  
985  
986  
987  
988  
989  
990  
991  
992  
993  
994  
995  
996  
997  
998  
999  
1000

1A-1

We subsequently greatly improved the femtosecond XeCl amplifier by substituting for the synch-pumped dye laser and fiber pulse compressor a *colliding-pulse mode-locked dye laser* (CPM) working at 616nm<sup>2</sup>. This system produced pulses of 160-fsec duration, the bandwidth limit<sup>2</sup> for XeCl. A simple *multiplexer* that was introduced<sup>3</sup> allowed the amplification of *two*, orthogonally polarized, 308-nm, 160-fsec pulses with each discharge of the excimer module used. The energy of each pulse is about 4 mJ when a single pass of amplification in an EMG101 module is used, and about 12 mJ when the seed passes through two such amplifiers. The apparatus runs very reliably over long periods of time, requiring a minimum of adjustment.

### 3. Continuum Generation in Gases

Following the successful development of an energetic, 160-fsec, 308-nm photolytic source, the main task of our group became to find ways in which femtosecond *continua* could be generated for use in *broadband absorption* probing of transition states produced by the photolytic action of the femtosecond 308-nm pulses. In a short period of time, we successfully discovered two separate techniques for producing such continua. These are now briefly described.

#### A. Generation of a Femtosecond IR (2.2-2.7 $\mu$ m) Continuum by Stimulated Electronic Raman Scattering in Ba Vapor.

We observed that a strong,  $\sim 1000\text{-cm}^{-1}$ -wide, 160-fsec continuum could be efficiently produced by focussing the amplified 308-nm pulses into Ba vapor<sup>4</sup>. The generating mechanism was shown to be transient stimulated electronic Raman scattering (SERS). It was also shown in Ref. 4 that the femtosecond IR continuum could be readily upconverted by four-wave mixing in an alkali metal vapor driven by a *nanosecond* laser. Thus, the stage was set for measurement of ultrafast events possessing spectral features in this wavelength range. Such an event was subsequently identified and measured (Sec. 4).

#### B. Generation of Femtosecond UV and Visible Continua in High Pressure Gases.

We also soon discovered<sup>3,5</sup> that a powerful *femtosecond UV continuum* extending from 230 to 400 nm (Fig. 1b) could be efficiently generated by focussing the amplified 308-nm pulses into a high pressure cell containing any one of a number of common laboratory gases-Ar, N<sub>2</sub>, CO<sub>2</sub>, etc. It immediately became evident that gas-phase continuum generation is the dominant nonlinear process in high-pressure gases in the *femtosecond* regime, completely displacing from this role stimulated Raman scattering, which is the dominant nonlinear process in the *picosecond* regime. The newly discovered effect appeared to be the gas-phase equivalent of the so-called "supercontinuum generation" phenomenon that occurs in condensed matter, an effect well known, and extensively utilized, by kinetic spectroscopists since 1970. However, *the gas-phase continuum driven at 308 nm contains much more light in the UV region than does a condensed matter continuum driven by a visible laser.* It should, therefore, in our opinion, in the long run be much more useful for femtosecond kinetic absorption spectroscopy of molecules and atoms than a visible continuum, because the majority of the atoms and molecules primarily absorb in the UV. It should here, of course, be mentioned that supercontinuum generation in the condensed phase simply does not work with 308-nm pumping. Thus, for UV work, the gas-phase continuum generation becomes virtually a necessity.

A *visible* gas-phase continuum, extending from 400 to 950 nm (Fig. 1c), can also easily be produced by focussing the amplified 616-nm pulses into the same high pressure gases. For convenience, we utilize this visible continuum when the transient spectral features being studied occur in the visible (see Sec. 6A).

To cancel the effects of random spectral variations appearing from shot to shot in either the visible or UV continuum, we incorporated a *reference channel* (see Fig. 2) in our apparatus<sup>6</sup>. This involved installation of a second OMA and spectrograph, both identical to the ones used in the signal channel. This gained for us more than a factor 10 in sensitivity.

The 308-nm-driven, high-pressure-gas, UV continuum also directly provides us with femtosecond seed pulses suitable for amplification at 248.5 nm in a KrF excimer gain module<sup>3,5</sup>. In this simple manner (Fig. 2), we directly obtain amplified pulses at 248.5 nm having 7-mJ pulse energy and 200-fsec pulse duration. These pulses are used for photolysis of molecules which do not absorb at 308 nm, such as the molecule DABCO, discussed immediately below.

#### 4. Measurement of Internal Conversion in DABCO Vapor: Use of the IR Continuum as Probe

An experiment (Fig. 3) utilizing the femtosecond 2.2-2.7  $\mu\text{m}$  continuum (sec. 3A) was performed in DABCO vapor<sup>7</sup>. This involved femtosecond pumping at 248.5 nm to the  $\tilde{B}$  state, internal conversion (IC) to vibrationally excited levels  $\tilde{A}^+$  of the  $\tilde{A}$  state, and probing via broadband IR absorption the  $\tilde{B}^+ \leftarrow \tilde{A}^+$  transition. The results (Figs. 4,5) showed that the  $\tilde{B} \rightarrow \tilde{A}^+$  IC process takes less than 0.5 psec. This experiment marked the first time femtosecond kinetic absorption spectroscopy was performed in the IR. Although our original technical proposal stressed the use of the IR spectral region for broadband transient spectroscopy, our subsequent inability to generate femtosecond IR continua outside the 2.2-2.7  $\mu\text{m}$  wavelength range (see Sec. 8) curtailed further investigations on our part in the IR. Instead, we began to concentrate on probing in the UV and visible regions, as we shall now discuss.

#### 5. Femtosecond Photolysis of Thallium Halide Vapors: Use of the UV Probe Continuum

In the past few years spectroscopic observation in real time of the "transition states" of a chemical reaction has become possible with the development of laser pulses as short as 6 femtoseconds. A.H. Zewail et al. have conducted femtosecond transition-state spectroscopy (FTS) experiments on several gas-phase photodissociation reactions involving either (1) direct dissociation<sup>8</sup> into the final photofragments that are produced or (2) predissociative trapping<sup>9</sup> of the photofragments en route to attainment of the final product distribution. In these FTS experiments, a femtosecond UV pump pulse first excites a molecule to a repulsive electronic state. A tunable femtosecond probe pulse, delayed by a variable time from the pump pulse, then detects one of the photofragments as it undergoes separation from the rest of the molecule, the probe pulse inducing either fluorescence (LIF) of the fragment or its multiphoton ionization (MPI) in a time-of-flight apparatus. Spectral changes that are observed in the (LIF) excitation spectrum at small pump-probe separations thus provide information about variations in the separation between the potential curves involved in the probe transition, occurring as the interatomic spacing is varied, with the photofragment still in the force field of the remaining parts of the molecule, i.e., with the whole photodissociating complex still in the process of passing through a continuous sequence of "transition states".

There is, of course, an alternative approach to the real time optical spectroscopic study of transition states produced by photodissociation, one which we have applied to the study of a number of systems during the recently completed contract period. In this approach, as in FTS experiments, a femtosecond UV pump source first excites a molecule to a repulsive electronic state. After a variable delay, a femtosecond probe pulse is also then applied. However, in this case, the probe pulse is one of our  $\sim 20,000 \text{ cm}^{-1}$  -wide *continuum* pulses, and the photofragments are detected via *broadband absorption spectroscopy*. A complete spectrum corresponding to a given pump-probe delay is thus recorded in a single shot. One now varies the pump-probe delay and notes how the appearance of the absorption spectra change, from the moment when absorption is first discerned, to the point at which no further changes in the spectra occur. These time-dependent absorption spectra form the data base for our approach to real time transition-state spectroscopy.

The first systems we chose to study with our technique of femtosecond broadband absorption spectroscopy were the TI-halides, TII and TlCl<sup>5,10</sup>. Unusual line shapes were observed (Fig. 6a) for a period lasting roughly 1 psec, from the moment the atomic transition first appears, to the point at which the final, asymptotic, line shape is attained. While the transient spectra obtained were all clearly identifiable as *atomic*, the striking asymmetries in line shapes that were observed clearly demonstrated that they were spectral signatures of *atoms still in the force fields of their receding partners*. Completely unanticipated by any of Zewail's published work was (1) the occurrence of transient spectra having the appearance of *gain* in certain spectral regions and (2) the observation that *the transient spectra all are centered about the asymptotic line positions*.

To explain the two above-mentioned unanticipated observations, our group developed a theory<sup>5,10</sup> that seems able to account for the main observed features of the transient spectra. This required use of a model for the transient polarization induced by the probe pulse. For an atom that is born at time  $t = t_i$  (alternatively, one can regard the oscillator strength of the atomic transition being probed as having a sharp onset at some internuclear separation,  $r_i$ , with the internuclear separation passing through this value in its trajectory at  $t = t_i$ ), the polarization induced by a delta function continuum pulse occurring at  $t = 0$  was shown<sup>5,10</sup> to have following time dependence:

$$\langle p(t, t_i) \rangle_B \sim e^2 |r_{10}|^2 \Pi(-t_i) \Pi(t - t_i) e^{-t^2/2\tau_B^2}$$



$$\times \exp\left(-\frac{i}{\hbar} \int_0^t [\delta E_1(t') - \delta E_0(t')] dt'\right), \quad (1)$$

where the  $\delta E_i$ 's denote deviations of the upper and lower levels being probed from their asymptotic values, and  $e r_{10}$  represents the transition dipole moment, which, in these calculations, is assumed to be a constant function of internuclear separation. In the above equation,  $H$  represents a Heaviside function. The quantity  $\gamma$  is a dephasing factor for the polarization introduced in the two-level atom Schrödinger equation. For simplicity,  $\gamma$  is assumed to be a constant function of internuclear separation. The quantity  $2/\tau_B$  represents the contribution to the asymptotic line width due to an unspecified source of inhomogeneous broadening<sup>5,10</sup>. Both  $\gamma$  and  $\tau_B$  are treated as adjustable parameters.

As shown in Refs. 5,10, it is the phase factor in Eq. (1) that is primarily responsible for the asymmetrical absorption profile observed. In Refs. 5,10 we assumed the following specific time dependence for the energy separation:

$$\frac{1}{\hbar} [E_1(t) - E_0(t)] = \omega_a^0 - \Delta\omega_R \left[ \exp\left(-\frac{t-t_i}{\tau_R}\right) \right], \quad (2)$$

where  $\omega_a^0$  is the unperturbed atomic transition frequency. Integration of Eq. (1) over a distribution function  $D(t) = dN(t)/dt$ , where  $N(t)$  represents the atomic population was also performed. We specified  $D(t)$  to be proportional to the quantity  $\text{sech}^2[(t-t_D)/\Delta t_D]$ . The quantity  $t_D$  is the separation between the pump and probe. The quantity  $\Delta t_D$  characterizes the width of the growth period. A lower limit to  $\Delta t_D$  would clearly be the pump pulse duration (160 fsec at 308 nm).

Results from the theoretical model are shown in Fig. 6b. The values of the five basic parameters chosen for this figure are:  $\gamma = 0.0003 \text{ fsec}^{-1}$ ,  $\Delta t_D = 150 \text{ fsec}$ ,  $\hbar\Delta\omega_R = 50 \text{ cm}^{-1}$ ,  $\tau_R = 300 \text{ fsec}$ , and  $\tau_B = 5000 \text{ fsec}$ . A qualitative agreement with the shape of the observed spectra is obtained. Note that the theoretical fit implies that the transition being probed is subject to a  $50 \text{ cm}^{-1}$  red shift at the internuclear separation ( $r_i$ ) at which the oscillator strength attains appreciable magnitude. With

the interatomic separation increasing at a rate  $\sim 7 \text{ \AA/psec}^{5,10}$ , the value  $\tau_R = 300 \text{ fsec}$  implies that the  $1/e$  decay length for the red shift is  $\sim 2 \text{ \AA}$ .

In Fig. 7, we plot the time decay of the amplitude of the induced polarization, computed with the use of our model. The relatively long time constant for light radiated by the induced polarization that is implied by this plot basically shows why the transient spectra we observe are "centered" about the asymptotic atomic line position. In Fig. 8, we plot trajectories for the electric field radiated by the induced polarization. This figure is in the form of a polar plot in which the radius represents the amplitude of the radiated field and the angle represents the phase of the radiated field relative to the probe. The time evolution of the radiated field is plotted for four of the traces shown in Fig. 6b. Note that, at long pump-probe delay times, as the radiated field decays, it remains always  $180^\circ$  out-of-phase with respect to the carrier frequency  $\omega_C$ . *At short delay times, however, there are large changes in the relative phase. These are responsible for the observed spectral asymmetries, including the appearance of transient gain in certain spectral regions.*

Other atomic transitions of TII, TlCl were probed in Refs. 5,10. A wide variety of transient asymmetries were observed. Some transitions exhibited quite unusual transient features. For example, in the case of TlCl, with 248-nm excitation, the 351.9-nm absorption line develops a pronounced transient *blue wing*. In all, the results presented in Refs. 5 and 10 suggest that a *new domain of atomic spectroscopy has been uncovered-that of atoms still in the force fields of their receding partners*- and that this domain exhibits a richness in the variety of line shapes displayed that, properly interpreted, reveals a great deal of information about the continuous sequence of "transition states" through which atoms evolve on their way to becoming free.

## 6. Results from Other Systems

### A. NaI

Gaseous NaI, when photodissociated in the 300-328 nm spectral region, undergoes a predissociative reaction. The wave packet prepared by the pump excitation is largely trapped in an adiabatic well, but it has a small probability ( $\sim 0.1$ ) of undergoing Landau-Zener tunneling onto the diabatic potential curve, thus permanently escaping the adiabatic well, each time the wave packet

approaches the curve-crossing region. With the use of their femtosecond LIF technique, Zewail's group has now experimentally observed in real time oscillations of the wave packet in the adiabatic well in this system.<sup>9</sup>

We have also examined the NaI system experimentally, utilizing our femtosecond kinetic absorption spectroscopy apparatus<sup>12</sup>. Photolysis was performed at both 248.5 and 308 nm. We discuss the 248.5-nm results first. Figure 9 shows a sequence of time-resolved absorption spectra obtained in the vicinity of the Na "D" lines when NaI was photolyzed with  $\sim 200$  fs pulses at 248.5 nm. The visible femtosecond gas-phase continuum (Fig. 1c) was used as a probe. It is seen that the Na absorption lines develop in a smooth manner, with no apparent asymmetries present. Some broadening of the spectra at early times is evident. The peak absorption coefficient is smoothly attained in  $\sim 1.5$  psec (Fig. 10). A determination of when the pump pulse occurs with respect to the growth curve in Fig. 10 was not made.

Substantially the same transient absorption line shapes are seen when NaI is photolyzed at 308 nm. Here the principal difference is that the growth of the Na "D" lines occurs in  $\sim 1$ -ps steps (Fig. 11). The curve presented in Fig. 11 is basically similar to the Na growth curve shown in Ref. 9 for on-resonance LIF excitation.

From the standpoint of the discussion presented in Sec. 5, the principal surprise contained in Fig. 9, and in the individual time-resolved spectra corresponding to Fig. 11, is the almost total *lack of asymmetry* present in the transient absorption spectra, particularly when compared to the case of the thallium halides. Yet this observation is in full agreement with the theoretical model presented in Sec. 5 for the following reason. It is known that the dissociative potential curves of NaI are extremely flat. For example, in Fig. 1 of Ref. 11, the diabatic potential energy curve  $E_3(r)$ , which leads to the fragments  $\text{Na}(^2P) + \text{I}(^2P_{3/2})$ , and which, therefore, corresponds to the upper level of the transition being probed in the case of Fig. 11 is drawn flat for much of the region of interest. The diabatic potential curve on which the photo-excited wave packet moves before approaching the avoided curve-crossing region, and after tunneling through it, is also drawn flat for  $r \geq 3.9\text{\AA}$ . (The avoided curve-crossing occurs at  $\sim 7.0\text{\AA}$ .) Thus, the red shift for Na atoms just formed must

*be close to zero.* No asymmetries in the transient spectra should, therefore, occur, according to Eq. (1).

The alkali halides may well represent a special case for the diatomics, in the sense that the changes in bonding that occur in these systems, when they are undergoing photodissociation, are comparatively simple. For example, photoexcitation of NaI at 308 nm from the bound ionic state  $E_1(r)$  to either the  $\Omega = 0^+$  or  $\Omega = 1$  dissociative surfaces transfers an electron from the iodine to the sodium, thus producing two adjacent neutral atoms which can then either directly dissociate ( $\Omega = 1$ ) or predissociate ( $\Omega = 0^+$ ) without requiring further dramatic changes in the chemical bonding. On the other hand, more electrons are involved in the bonding of thallium iodide, for example, so even if charge transfer of a single electron occurs from iodine to thallium in the photoexcitation of TlI to a dissociative surface, the remaining electrons involved in bonding will have to undergo drastic changes in their electronic configurations before the atoms are permanently separated. From this standpoint, perhaps, one can understand the meaning of a sudden 'turning on' of an atomic transition oscillator strength as a complex diatomic molecule undergoes photodissociation.

### B. Cyclopentadienyl thallium

In the organometallic compound Tl-cyclopentadienyl the Tl atom is axially positioned 3Å from the plane of the cyclopentadienyl radical. For this molecule, in the vapor phase, we have observed<sup>12</sup> that a 160-fs, 308-nm photolysis pulse dissociates the Tl atom from its cyclopentadienyl partner. Absorption spectra recorded with femtosecond resolution in the vicinity of the Tl 377.6-nm and 351.9-nm lines following the photolysis pulse again reveal unusual line shapes, similar to those found in Tl halide photodissociation (Fig. 12).

The spectra obtained in the photodissociation of Tl-cyclopentadienyl vapor begin to show evidence of another important transient effect we have discovered, namely, the enhancement of the Tl absorption coefficient at early times in the dissociation. This effect can, in retrospect, also be seen in Fig. 6a. However, no evidence of it is seen in the Na "D" line spectra resulting from photolysis of NaI (Figs. 9-11). The maximum transient enhancement of the absorption coefficient

in the case of Tl-cyclopentadienyl is a function of the relative polarizations of the pump and probe (Table 1). We will describe a system displaying a much stronger transient enhancement of the absorption coefficient in Sec. 6D.

### C. ICN

During the present contract period our group recorded spectrally well-resolved, time-dependent absorption spectra of CN radicals formed as a result of photolysis of ICN vapor by 200-fsec pulses<sup>12</sup>. With 248-nm pumping (Fig. 13), two groups of CN radicals are formed, one with very high, the other with very low rotational excitation. With 308-nm pumping, only one (medium excitation) CN rotational distribution is created. Although the existence of these nascent distributions was already well known, our results show that they are fully determined in less than 200 fsec, the time resolution of the apparatus. The actual growth of the CN population occurs in about 300 fsec (Fig 14). However, by the start of the rise, the rotational distributions have already been determined, and they do not change further. Note that the rotational lines appearing in Fig. 13 are comparatively sharp, much sharper than the  $\sim 30 \text{ cm}^{-1}$  spectral width one would associate with a 300 fsec risetime. The resolution of this paradox is that the spectral width of the recorded absorption bands can be shown to depend essentially on the *fall-time* of the polarization induced by the probe pulse, and *not* on its *rise-time*. A fast rise-time contributes intensity to the far wings of the bands, but at a level  $\sim 1000\times$  down from the peak, and hence, practically speaking, unobservable.

### D. Bismuth ( $\text{Bi}_2$ )

Our group has recently applied femtosecond transition-state spectroscopy to the UV photolysis of  $\text{Bi}_2$  molecules contained in bismuth vapor<sup>13</sup>. The small release of kinetic energy during photodissociation and large mass of the Bi atom both lead to a low Bi-Bi separation velocity. This makes the photodissociation of  $\text{Bi}_2$  a model system for transition-state absorption spectroscopy of diatomic molecules. The principle novel findings of this study can be summarized as follows. (1) With excitation at 308 nm ( $\sim 32460 \text{ cm}^{-1}$ ), at least two dissociative channels (M and M' in Fig. 15) are observed to be active, each channel producing both a ground state atom ( $^4\text{S}_{3/2}$ ) and an excited state atom ( $^2\text{D}_{3/2}$  or  $^2\text{D}_{5/2}$ ). (2) Formation of  $^2\text{D}_{3/2}$  atoms is observed to be *delayed* in time by

$\sim 0.5$  psec with respect to formation of  $^2D_{3/2}$  atoms. (3) *Asymmetric transient absorption line shapes* are observed for five different UV atomic transitions monitoring the populations of the  $^2D_{3/2}$  and  $^2D_{5/2}$  states. These spectra are qualitatively explained in terms of the model which was discussed in Sec. 5 and which is based upon the transient behavior of the polarization induced by the probe continuum pulse as it interacts with a growing population of two-level atoms whose resonance frequencies shift in time. (4) *Transient enhancements of the atomic absorption coefficients* are also observed for all these transitions. In one particular case (Fig. 16) the enhancement is especially dramatic ( $> 3\times$ ). Furthermore, it is found that for these transitions, *attainment of the asymptotic atomic configuration for the upper state wavefunction occurs at differing internuclear separations*. Interpretation of such complex behavior awaits detailed quantum chemistry calculations which not only address potential energy curves, but also the magnitude of the transition moment as a function of the internuclear separation. The unanticipated richness in the transient spectra we have thus far observed hopefully will turn the attention of theorists towards this new domain of spectroscopy.

## 7. Summary

Under contract DAAL03-86-C-0008, an apparatus for performing femtosecond transition-state absorption spectroscopy has been developed. The UV pump pulses rely upon amplification of femtosecond pulses in excimers. The probe pulses rely upon gas-phase continuum generation. Both effects were first realized and/or discovered by our group during the contract period just completed.

With the above apparatus, femtosecond transition-state absorption spectroscopy has been performed on Tl, Na, and Bi atoms produced by the 308-nm and 248-nm photodissociation of various gas-phase molecules, and also on CN radicals produced by UV photolysis of ICN. In the case of Tl and Bi, the transient spectra obtained are all clearly identifiable as *atomic*, yet they display striking asymmetries in line shapes and enhancements in intensity that clearly demonstrate that they are spectral signatures of atoms still in the force fields of their receding partners. A new area of spectroscopy has thus been defined.

## 8. Addendum: The Non-Realized Goals

In our original contract proposal, an emphasis was placed upon the discovery of techniques for producing continua in the IR ("subpicosecond TRISP"). We had assumed that such continua could readily be produced with various cascaded Raman shifting schemes involving both stimulated Raman scattering (SRS) in high-pressure molecular gases and stimulated electronic Raman scattering (SERS) in metal vapors. What we learned, instead, during the just completed contract period, was that, in the femtosecond regime, the occurrence of SRS is almost totally supplanted by continuum generation. We also attempted SERS in a variety of metal vapors (Ba, Bi, Na, K, Sr, Tl, Tm) with use of both 308-nm and 248-nm pumping. Of these, only Ba and Tl worked. Pumping Ba with 308-nm resulted in the strong 2.2-2.7  $\mu\text{m}$  continuum (Sec. 3A), while Tl gave a strong Raman Stokes output at  $\sim 1.64 \mu\text{m}$  when pumped with 200-fsec, 248.5-nm pulses. Neither IR wavelength range is really in the vibrational "fingerprint" region. Thus, we quickly focussed upon the use of UV and visible continua, as has already been detailed.

With regard to the interesting, but highly speculative proposal we had made for an optical chain reaction (OCR) in  $\text{CO}(\text{N}_3)_2$ , we *did* make an attempt to drive infrared multiphoton dissociation (IRMPD) with a  $\text{CO}_2$  TEA laser to see if laser action on the CO vibrational transitions could be made to occur. Plenty of  $\sim 5 \mu\text{m}$   $\text{CO}^*$  fluorescence was recorded, but no laser action was observed. Our conclusion was that the  $\text{CO}^*$  population produced by decomposition of the parent molecule was probably not inverted. In this system, it may be the vibrationally excited nitrogen that is inverted. These hypotheses will undoubtedly be tested sometime in the future, when it becomes possible to probe the spectral regions required.

**Table 1. Maximum Transient Enhancements of T1 Absorption Coefficients Observed for 308-nm Photolysis**

	Pump $\perp$ Probe	Pump $\parallel$ Probe
T1 351.9	2.1	1.5
T1 377.6	1.0	1.6



## REFERENCES

1. J.H. Glowia, G. Arjavalingham, P.P. Sorokin, and J.E. Rothenberg, "Amplification of 350-fsec Pulses in XeCl Excimer Gain Modules", *Opt. Lett.* 11, 79 (1986).
2. J.H. Glowia, J. Misewich, and P.P. Sorokin, "160-fsec XeCl Excimer Amplification System", *J. Opt. Soc. Am. B* 4, 1061 (1987).
3. J.H. Glowia, J. Misewich, and P.P. Sorokin, "Ultrafast Ultraviolet Pump-Probe Apparatus", *J. Opt. Soc. Am. B* 3, 1573 (1986).
4. J.H. Glowia, J. Misewich, and P.P. Sorokin, "Subpicosecond Time-resolved Infrared Spectral Photography", *Opt. Lett.* 12, 19 (1987).
5. J.H. Glowia, J. Misewich, and P.P. Sorokin, "Utilization of UV and IR Supercontinuum in Gas-Phase Subpicosecond Kinetic Spectroscopy", in The Supercontinuum Laser Source, edited by R.R. Alfano. Springer-Verlag, New York, 1989.
6. J.H. Glowia, J. Misewich and P.P. Sorokin, "The Utilization of UV and IR Supercontinua in Gas-Phase Subpicosecond Kinetic Spectroscopy", in Proceedings of the Electrochemical Society: Nonlinear Optics and Ultrafast Phenomena, ed. by L. Rothberg and R.R. Alfano (in press).
7. J.H. Glowia, J. Misewich, and P.P. Sorokin, "Subpicosecond IR Transient Absorption Spectroscopy: Measurement of Internal Conversion Rates in DABCO Vapor", *Chem. Phys. Lett.* 139, 491 (1987).
8. M. Dantus, M.J. Rosker, and A.H. Zewail, *J. Chem. Phys.* 87, 2395 (1987).
9. M.J. Rosker, T.S. Rose, and A.H. Zewail, *Chem. Phys. Lett.* 146, 175 (1988).
10. J. Misewich, J.H. Glowia, J.E. Rothenberg, and P.P. Sorokin, "Subpicosecond UV Kinetic Absorption Spectroscopy: Photolysis of Thallium Halide Vapors", *Chem. Phys. Lett.* 150, 374 (1988).
11. S.-Y. Lee, W.T. Pollard, and R.A. Mathies, *J. Chem. Phys.* 90, 6146 (1989).
12. J. Misewich, J.H. Glowia, and P.P. Sorokin, to be published.
13. J.H. Glowia, J.A. Misewich and P.P. Sorokin, "Femtosecond Transition-State Absorption Spectroscopy of Bi Atoms Produced by Photodissociation of Gaseous Bi<sub>2</sub> Molecules", submitted to *J. Chem. Phys.*

## FIGURE CAPTIONS

- Fig. 1a** Spectrum of Ba Raman Stokes light, recorded with the use of a scanning monochrometer and PbS detector.
- Fig. 1b** Spectrum of femtosecond, gas-phase, UV continuum.
- Fig. 1c** Spectrum of femtosecond, gas-phase, visible continuum.
- Fig. 2** Diagram of existing 160-fsec kinetic absorption spectrometer, configured for 248-nm UV pumping, and broadband UV probing.
- Fig. 3** Diagram of photophysical processes involved in the subpicosecond DABCO experiment.
- Fig. 4** (a) Absorbance (base 10) with probe delayed  $\approx 4$  psec with respect to pump. (b) Absorbance with probe pulse preceding pump pulse.
- Fig. 5** Peak  $\tilde{B}^+ \leftarrow \tilde{A}^+$  absorbance as a function of pump-probe delay time.
- Fig. 6** (a) Time-resolved absorption spectra recorded in the vicinity of the 377.6-nm Tl resonance line, following the application of 160-fsec, 308-nm pump pulses to TlI vapor. (b) Calculated transient absorption spectra. The relative pump-probe separation is indicated on the right.
- Fig. 7** Time dependence of the amplitude of the induced polarization, corresponding to the trace in Fig. 6b with a pump-probe separation 0.2 psec.
- Fig. 8** Plot of amplitude of the electric field radiated by the induced polarization, and its phase relative to the carrier frequency  $\omega_C$ . Trajectories corresponding to four traces in Fig. 6b are shown.

- Fig. 9** Time-resolved absorption spectra recorded in the vicinity of the Na "D" lines when NaI is photolyzed with  $\sim 200$ -fsec pulses at 248.5 nm. Between each spectrum the pump-probe separation was increased by 100 fsec.
- Fig. 10** Growth in time of Na absorption peak at  $\sim 589$  nm, following photolysis by  $\sim 200$ -fsec, 248.5-nm pulses.
- Fig. 11** Growth in time of Na absorption peak at  $\sim 589$  nm, following photolysis of NaI by 160-fsec, 308-nm pulses.
- Fig. 12** Time resolved absorption spectra recorded in the vicinity of the Tl 377.6-nm line after photolysis of Tl-cyclopentadienyl vapor with a 160-fsec, 308-nm pulse. Parallel pump, probe polarizations. Between each spectrum, the pump-probe separation was increased by 100 fsec.
- Fig. 13** Absorption spectrum of CN ( $B^2\Sigma^+ \leftarrow X^2\Sigma^+$ , 0-0 band), recorded 1 psec after application of 200-fsec, 248-nm photolysis pulse to ICN vapor.
- Fig. 14** Growth of CN absorption spectrum following application of 200-fsec, 248-nm photolysis pulse to ICN vapor. Absorption measured at peak of the P-branch band head.
- Fig. 15** Electronic states of  $\text{Bi}_2$  as represented in G. Gerber and H.P. Broida, J. Chem. Phys. 64, 3423 (1976). The dashed curve ( $M'$ ) is schematically drawn as a result of our work (see text).
- Fig. 16** Transient absorption spectra taken in the vicinity of the Bi lines near 299.0, 299.3 nm. 100 fsec between successive spectra. Perpendicular pump, probe polarizations. Asymptotic line shapes not yet fully attained in this sequence.

## PUBLICATIONS

The following list enumerates the publications by our group during the just completed contract period.

1. J.H. Glowina, G. Arjavalingham, P.P. Sorokin, and J.F. Rothenberg, "Amplification of 350-fsec Pulses in XeCl Excimer Gain Modules", *Opt. Lett.* 11 , 79 (1986).
2. J.H. Glowina, J. Misewich, and P.P. Sorokin, "Ultrafast Ultraviolet Pump-Probe Apparatus", *J. Opt. Soc. Am. B* 3 , 1575 (1986).
3. J.H. Glowina, J. Misewich, and P.P. Sorokin, "Amplification in a XeCl Excimer Gain Module of 200-fsec UV Pulses Derived from a Colliding Pulse Mode-Locked (CPM) Laser System", *J. Opt. Soc. Am. A.* 3 , 126 (1986).
4. J.H. Glowina, J. Misewich, and P.P. Sorokin, "New Excitation and Probe Continuum Sources for Subpicosecond Absorption Spectroscopy", in Ultrafast Phenomena V , edited by G.R. Fleming and A.E. Siegman, (Springer-Verlag, New York, 1986) p. 153.
5. J.H. Glowina, J. Misewich and P.P. Sorokin, "Subpicosecond Time-Resolved Infrared Spectral Photography", *Opt. Lett.* 12 , 19 (1987).
6. J.H. Glowina, J. Misewich and P.P. Sorokin, "Amplification in a XeCl Excimer Gain Module of 200-fsec UV Pulses Derived from a Colliding Pulse Mode-Locked (CPM) Laser System, *Proc. SPIE - Int. Soc. Opt. Eng.* 710 , 92 (1987).
7. J.H. Glowina, J. Misewich and P.P. Sorokin, "160-fsec XeCl Excimer Amplifier System", *J. Opt. Soc. Am. B* 4 , 1061 (1987).
8. J.H. Glowina, J. Misewich and P.P. Sorokin, "Subpicosecond IR Transient Absorption Spectroscopy: Measurement of Internal Conversion Rates in DABCO Vapor", *Chem. Phys. Lett.* 139 , 491 (1987).
9. J.H. Glowina, J. Misewich and P.P. Sorokin, "Subpicosecond UV/IR Absorption Spectroscopy", in Atomic and Molecular Processes with Short Intense Laser Pulses , ed. by A. Bandrank (Plenum, New York, 1988) p. 359.

10. J. Misewich, J.H. Glowia, J.E. Rothenberg, and P.P. Sorokin, "Subpicosecond UV Kinetic Spectroscopy: Photolysis of Thallium Halide Vapors", *Chem. Phys. Lett.* 150 , 374 (1988).
11. J.H. Glowia, J. Misewich and P.P. Sorokin, "The Utilization of UV and IR Supercontinua in Gas-Phase Subpicosecond Kinetic Spectroscopy", in The Ultrafast Supercontinuum Laser Source, ed. by R.R. Alfano (Springer-Verlag, Berlin, 1989).
12. J.H. Glowia, J. Misewich, J.E. Rothenberg and P.P. Sorokin, "Subpicosecond UV Kinetic Absorption Spectroscopy", *Optics News* 14 , 10 (1988).
13. J.H. Glowia, J. Misewich and P.P. Sorokin, "The Utilization of UV and IR Supercontinua in Gas-Phase Subpicosecond Kinetic Spectroscopy", in Proceedings of the Electrochemical Society: Nonlinear Optics and Ultrafast Phenomena, ed. by I. Rothberg and R.R. Alfano (in press).
14. J.H. Glowia, J.A. Misewich, and P.P. Sorokin, "Time-Resolved Transition-State Spectroscopy", in Proc. Ninth International Conf. on Laser Spectroscopy , edited by M. Feld (Academic Press, 1989), in press.
15. J.H. Glowia, J.A. Misewich, and P.P. Sorokin, "Femtosecond Transition-State Absorption Spectroscopy of Bi Atoms Produced by Photodissociation of Gaseous Bi<sub>2</sub> Molecules", submitted to *J. Chem. Phys.*

## ORAL PRESENTATIONS

The following list enumerates the oral presentations (made or to be made) by our group of ARO-supported work performed during the just completed contract period.

Institution or Conference	Place	Date	Invited (I) or Contributed (C)	Publications Resulting
OSA Annual Meeting	Washington, DC	October 1985	C	No
IQEC'86	San Francisco, CA	June 1986	C	No
Ultrafast Phenomena V	Snowmass, CO	June 1986	C	Yes
SPIE	Boston, MA	September 1986	I	Yes
OSA Annual Meeting	Seattle, WA	October 1986	C*	No
CLEO'87	Baltimore, MD	May 1987	C	No
Ford Research Center	Dearborn, MI	June 1987	I	No
NATO Workshop	Lennoxville, Que.	July 1987	I	Yes
OSA Annual Meeting	Rochester, NY	October 1987	I	No
OSA Annual Meeting	Rochester, NY	October 1987	I	No
CLEO'88	Anaheim, CA	April 1988	C	No
Electrochemical Society Annual Meeting	Chicago, IL	October 1988	I	Yes
NBS	Gaithersburg, MD	December 1988	I	No
Bookhaven	Upton, NY	January 1989	I	No
IQEC'89	Baltimore, MD	May 1989	I	No
NICOLS	Bretton Woods, NH	June 1989	I	Yes
Harvard	Cambridge, MA	November 1989	I	No
MIT	Cambridge, MA	December 1989	I	No

\*Indicates post-deadline paper

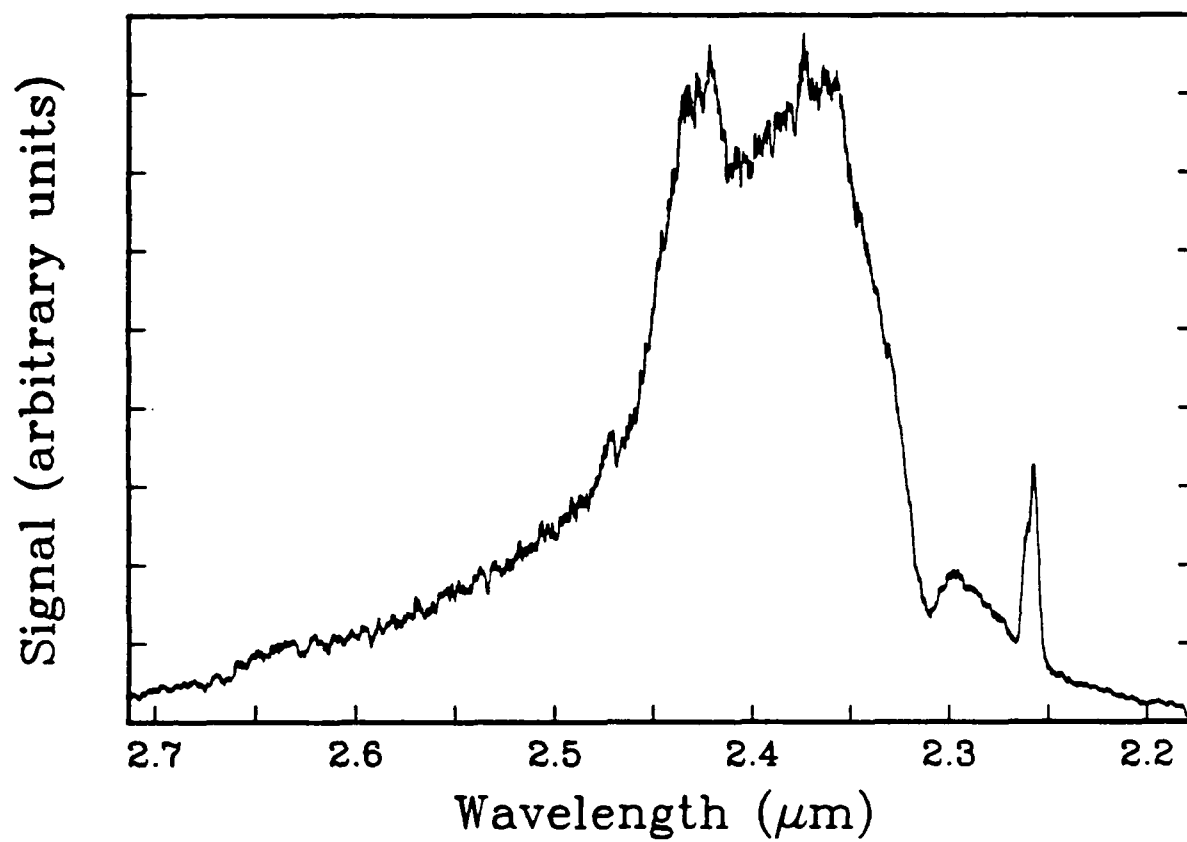


**Fig. 1a**      Spectrum of Ba Raman Stokes light, recorded with the use of a scanning monochromator and PbS detector.

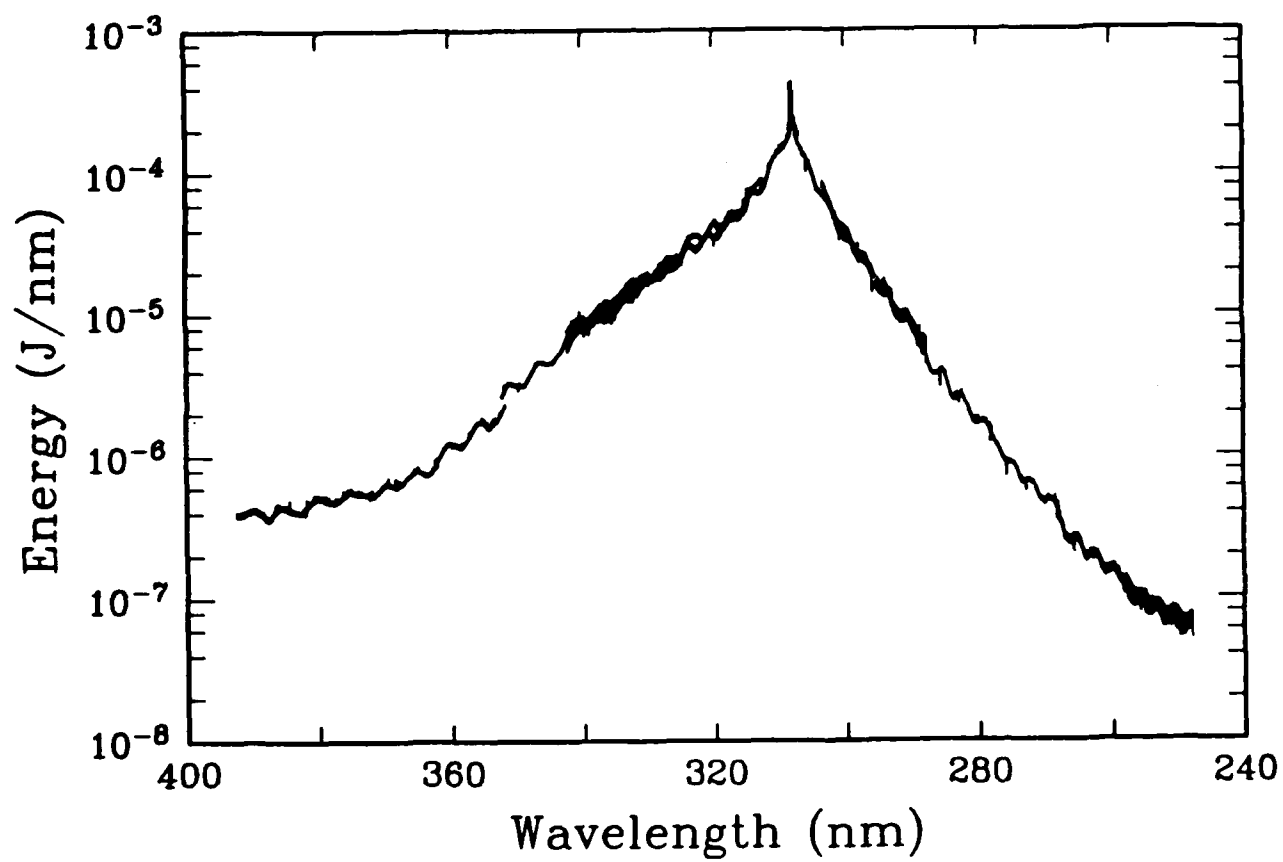


**Fig. 1b** Spectrum of femtosecond, gas-phase, UV continuum.



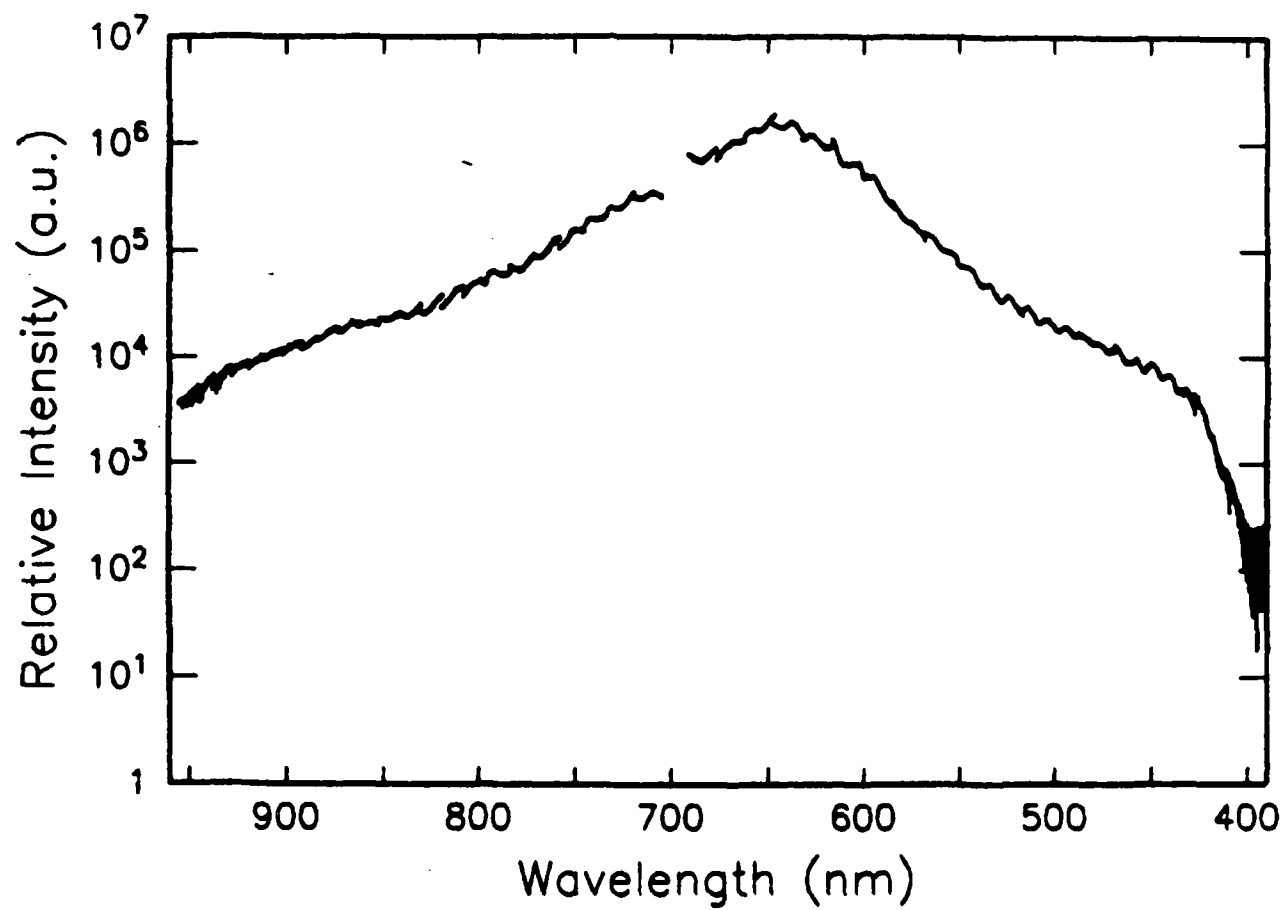


**Fig. 1c** Spectrum of femtosecond, gas-phase, visible continuum.

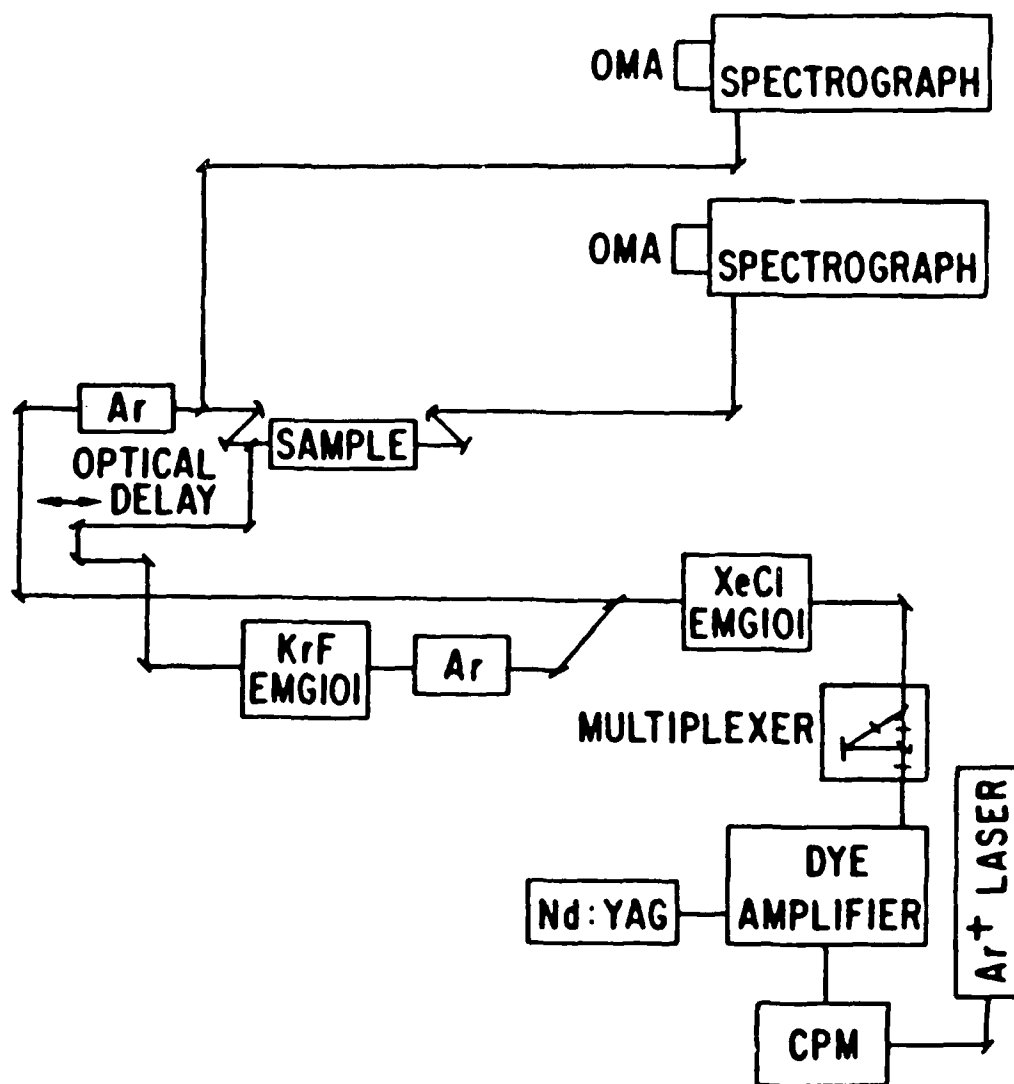


**Fig. 2** Diagram of existing 160-fsec kinetic absorption spectrometer, configured for 248-nm UV pumping, and broadband UV probing.

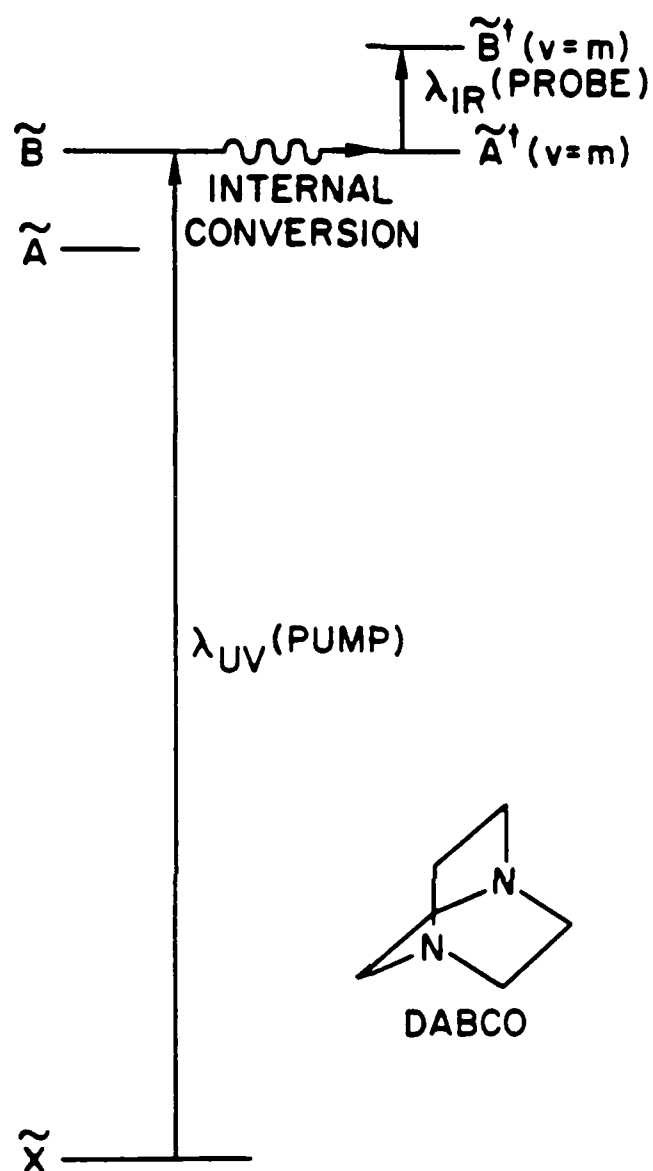


**Fig. 3** Diagram of photophysical processes involved in the subpicosecond DABCO experiment.

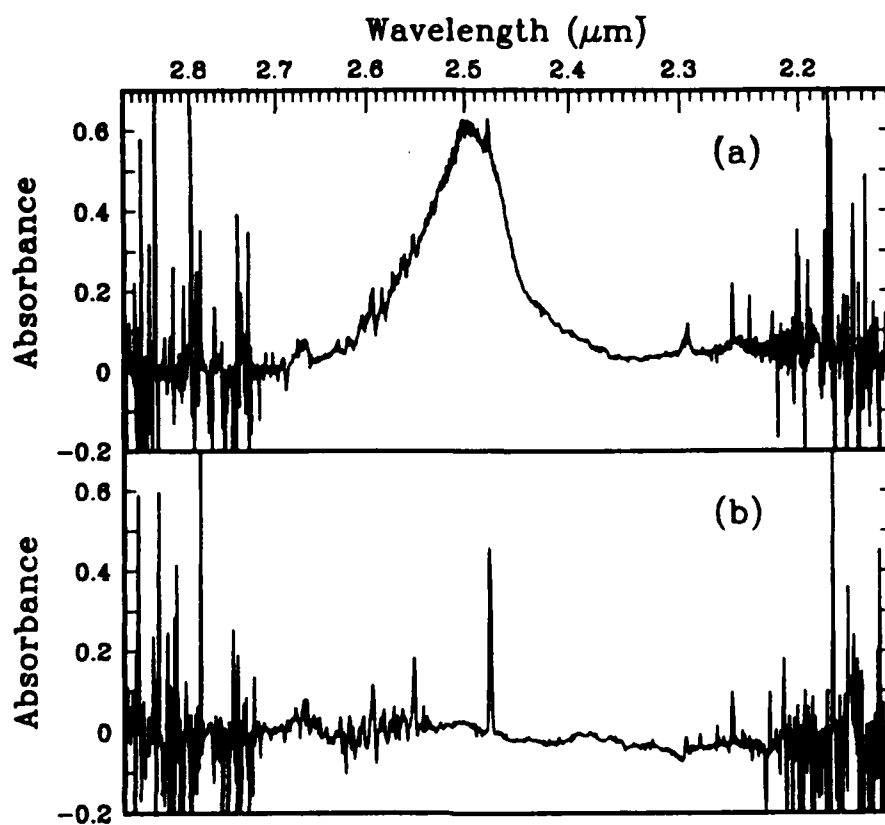


**Fig. 4** (a) Absorbance (base 10) with probe delayed  $\approx 4$  psec with respect to pump. (b) Absorbance with probe pulse preceding pump pulse.

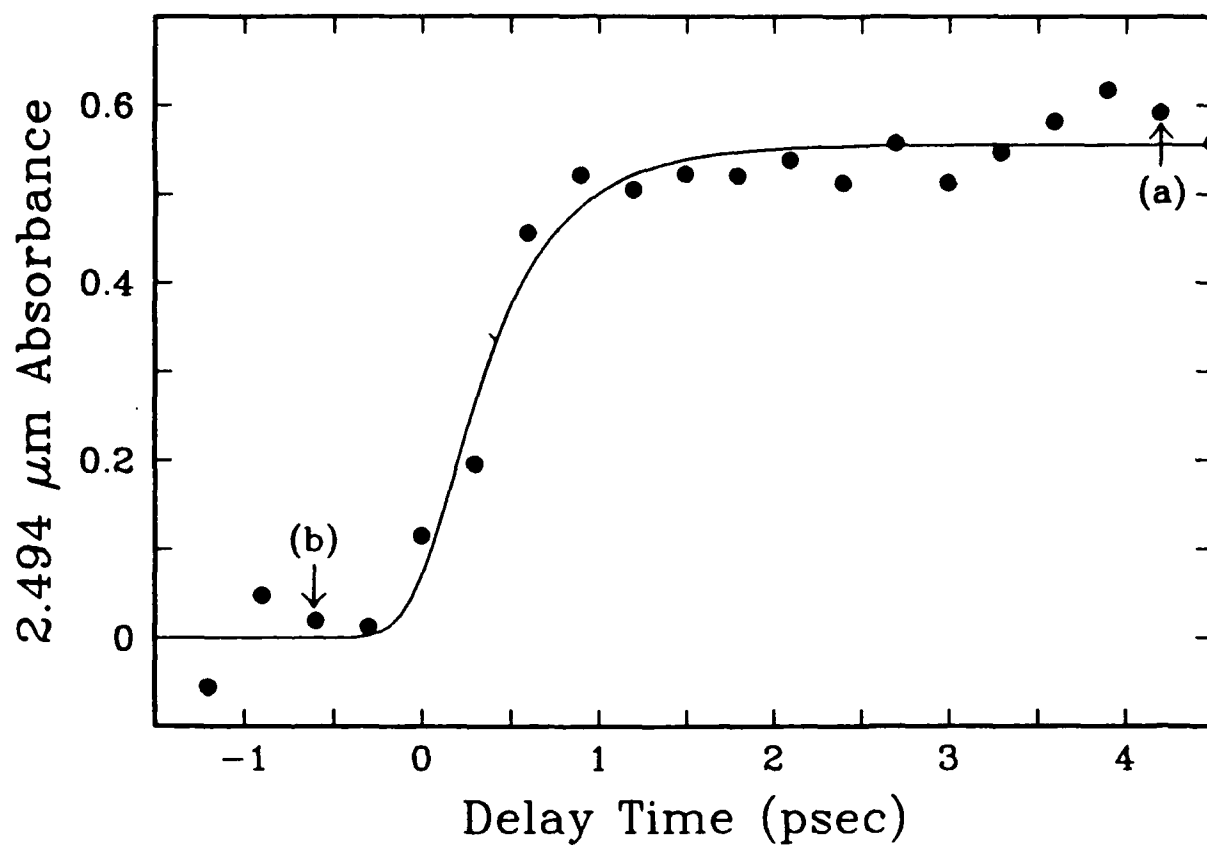


**Fig. 5** Peak  $\tilde{B}^+ \leftarrow \tilde{A}^+$  absorbance as a function of pump-probe delay time.

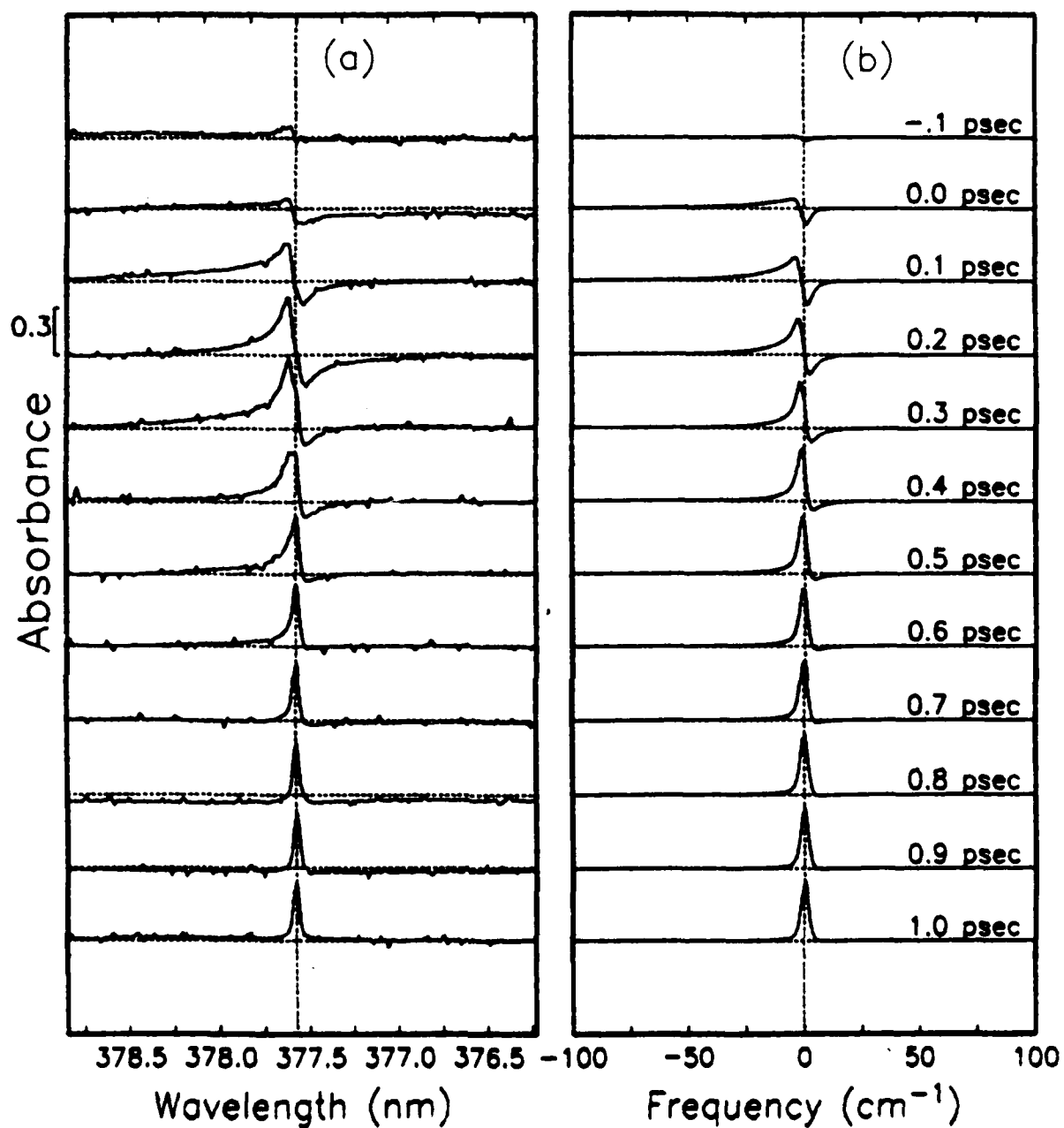


**Fig. 6** (a) Time-resolved absorption spectra recorded in the vicinity of the 377.6-nm TI resonance line, following the application of 160-fsec, 308-nm pump pulses to TI vapor. (b) Calculated transient absorption spectra. The relative pump-probe separation is indicated on the right.

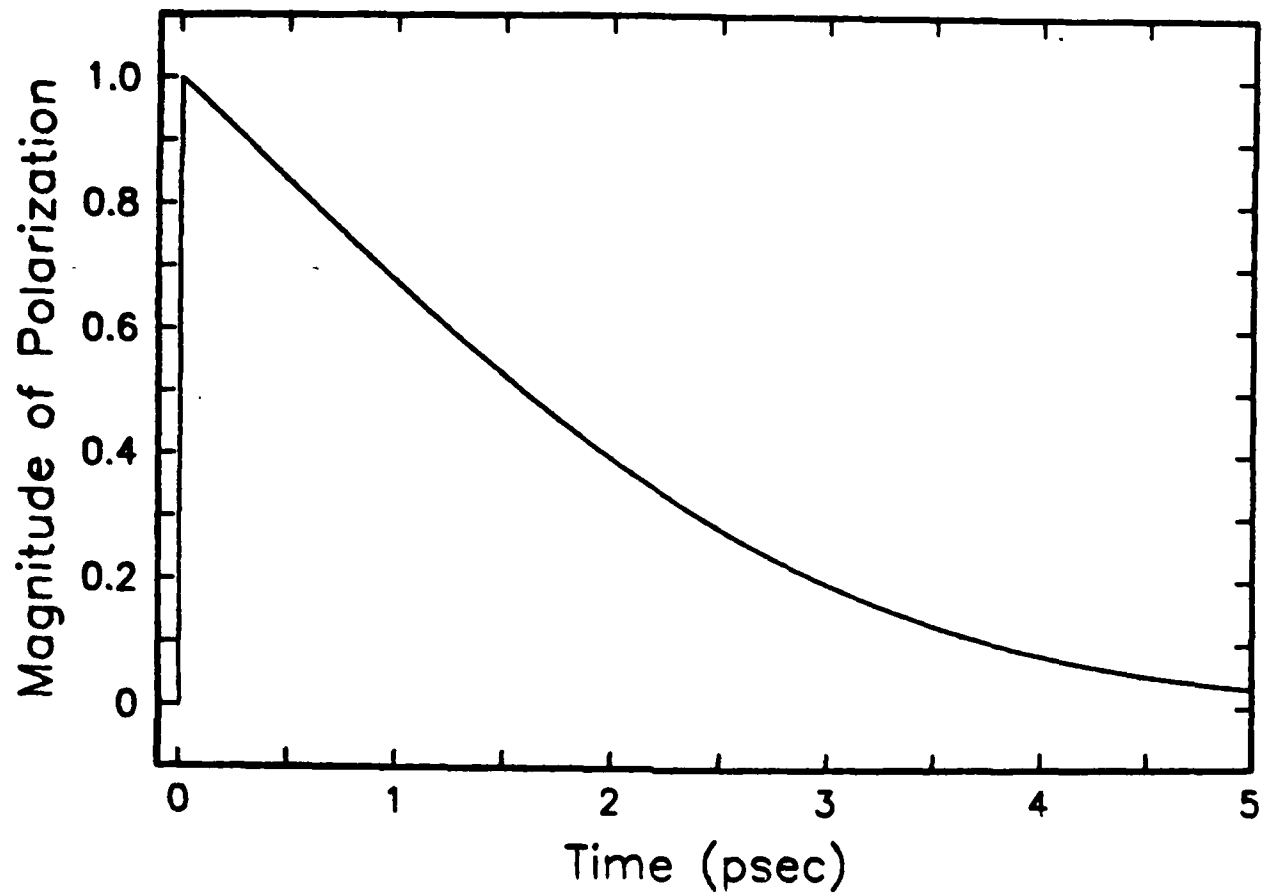


**Fig. 7** Time dependence of the amplitude of the induced polarization, corresponding to the trace in Fig. 6b with a pump-probe separation 0.2 psec.

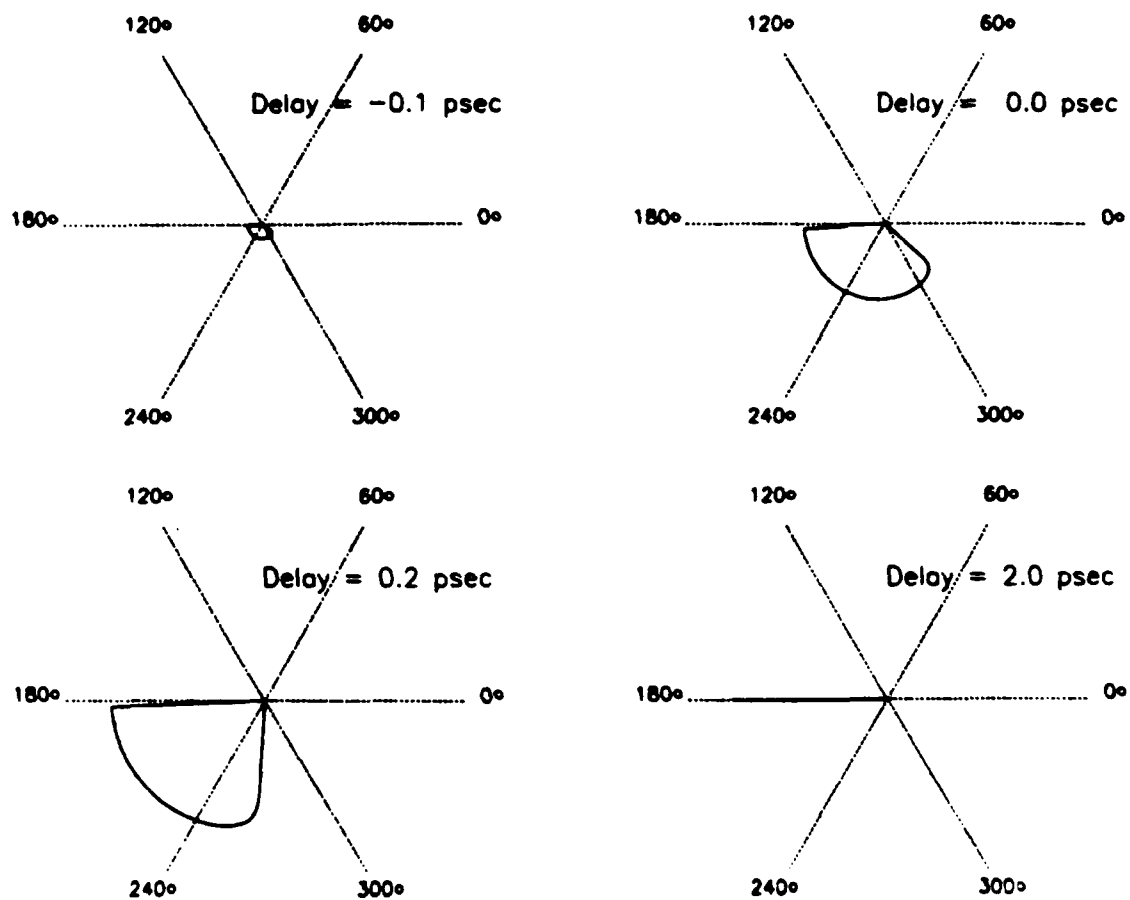


**Fig. 8** Plot of amplitude of the electric field radiated by the induced polarization, and its phase relative to the carrier frequency  $\omega_c$ . Trajectories corresponding to four traces in Fig. 6b are shown.



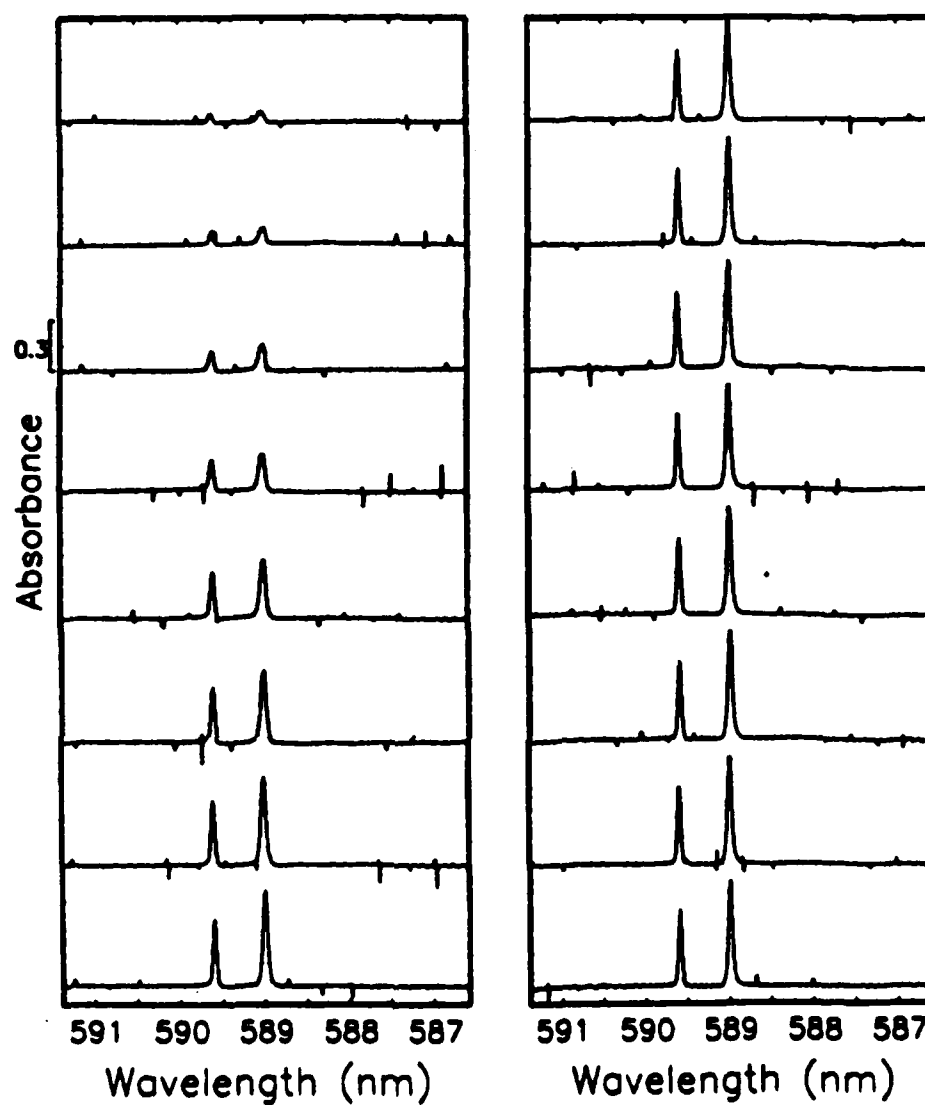


**Fig. 9** Time-resolved absorption spectra recorded in the vicinity of the Na "D" lines when NaI is photolyzed with  $\sim 200$ -fsec pulses at 248.5 nm. Between each spectrum the pump-probe separation was increased by 100 fsec.

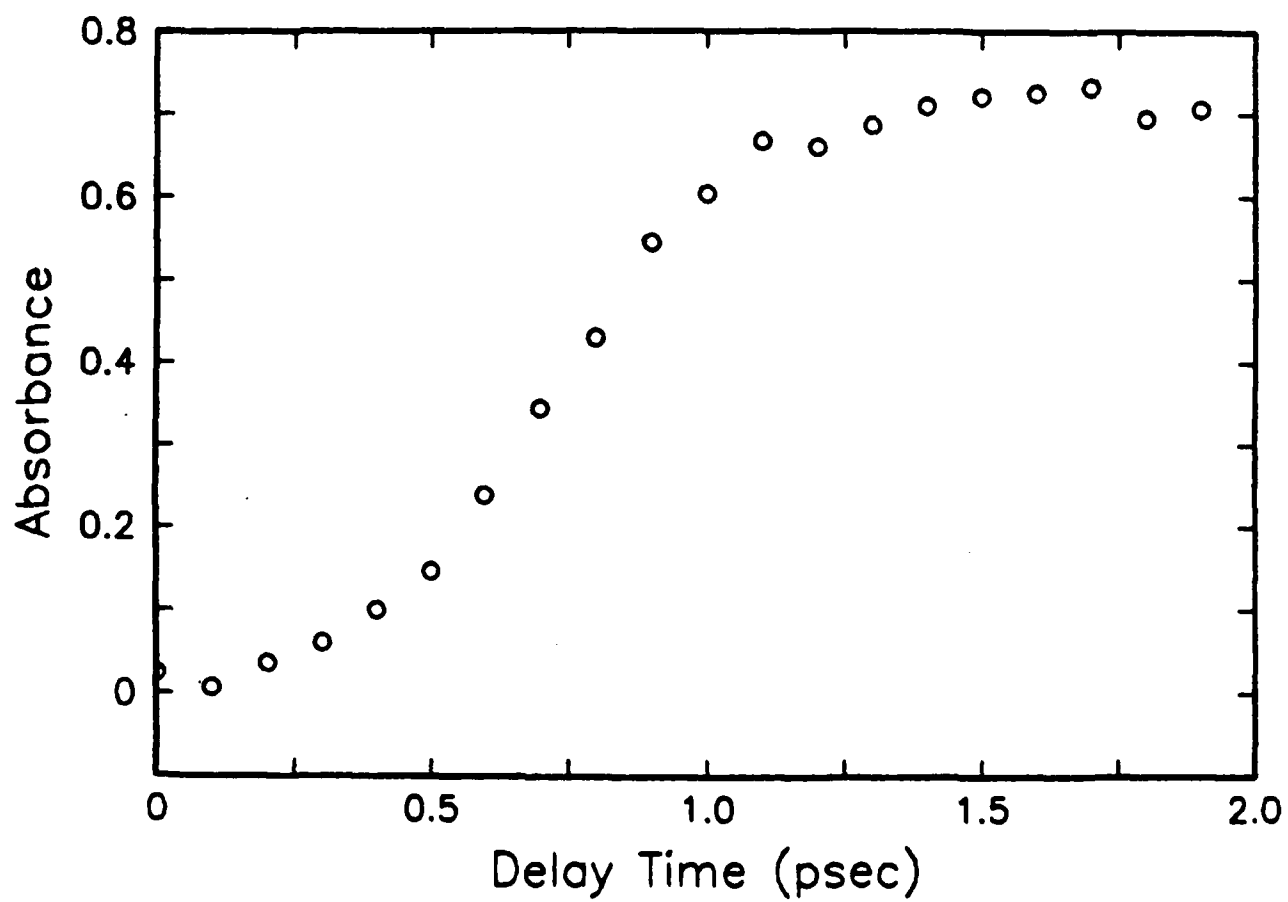


**Fig. 10** Growth in time of Na absorption peak at  $\sim 589$  nm, following photolysis by  $\sim 200$ -fsec, 248.5-nm pulses.

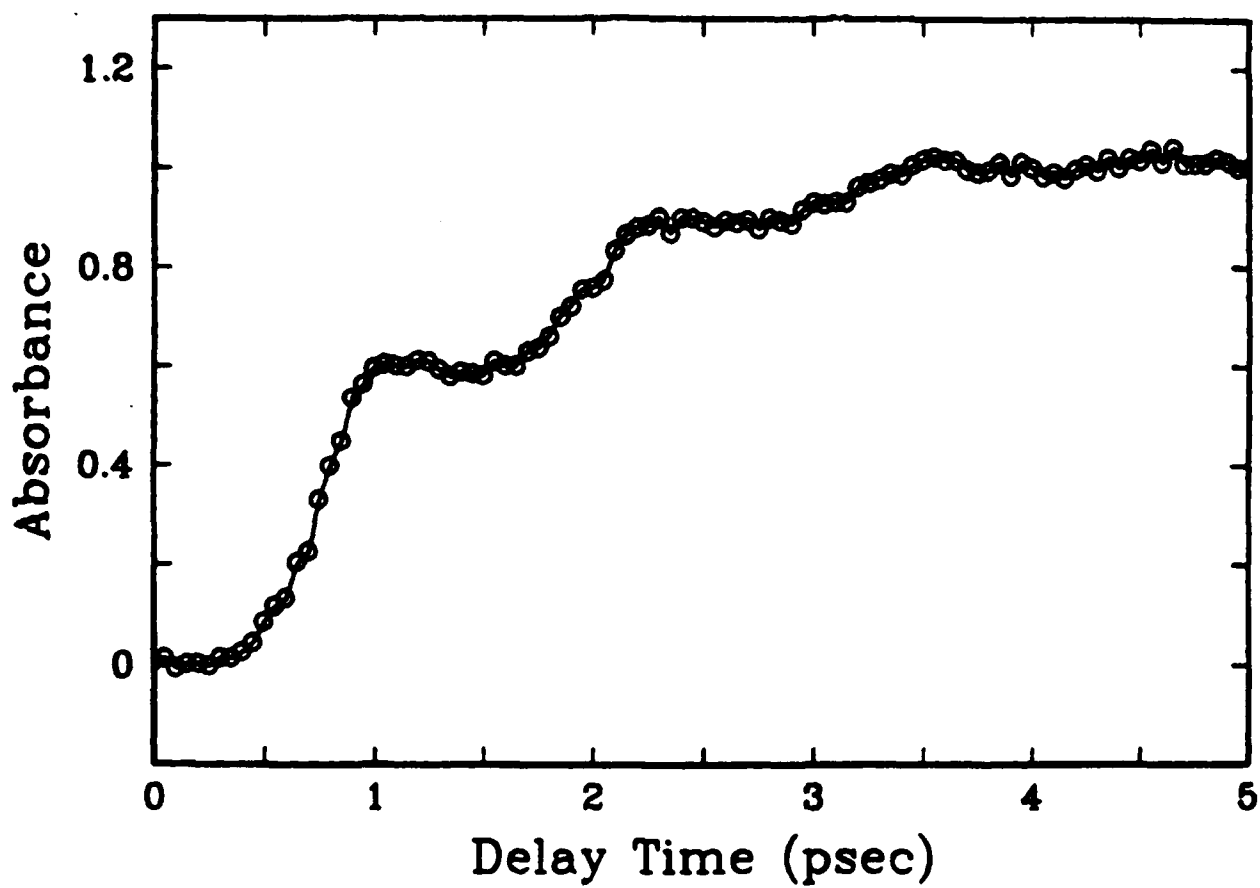


**Fig. 11** Growth in time of Na absorption peak at  $\sim 589$  nm, following photolysis of NaI by 160-fsec, 308-nm pulses.

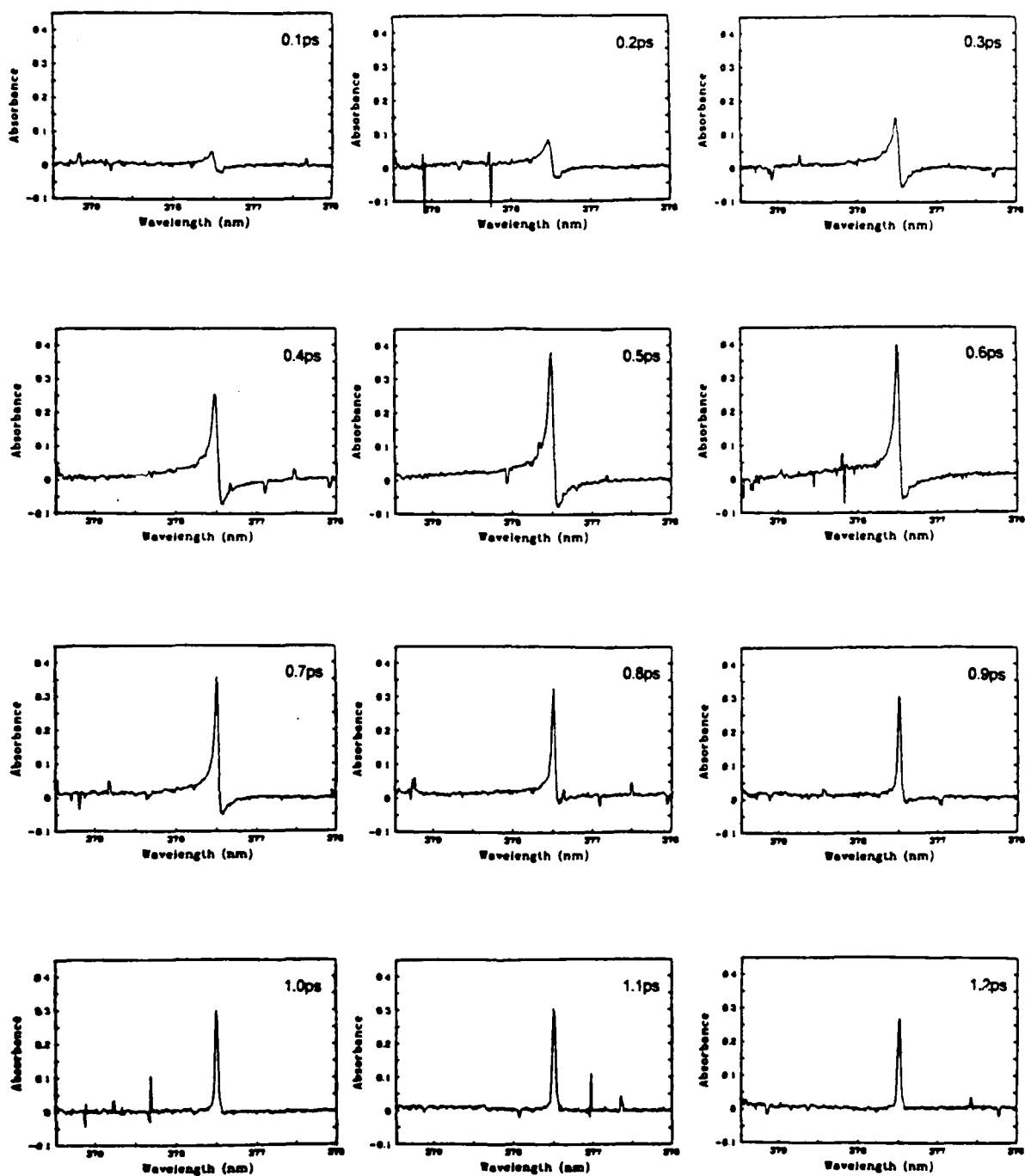


**Fig. 12**

Time resolved absorption spectra recorded in the vicinity of the Tl 377.6-nm line after photolysis of Tl-cyclopentadienyl vapor with a 160-fsec, 308-nm pulse. Parallel pump, probe polarizations. Between each spectrum, the pump-probe separation was increased by 100 fsec.

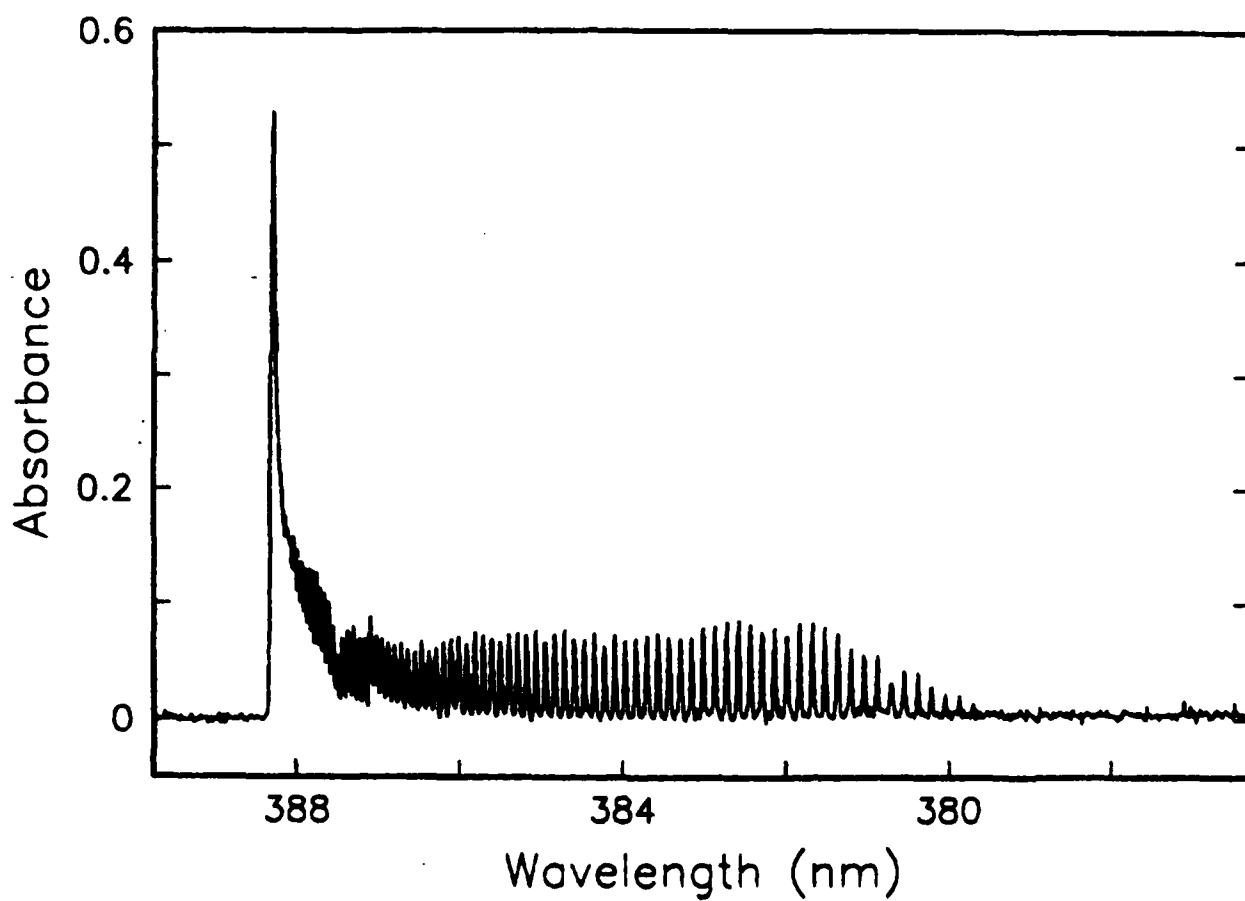


**Fig. 13** Absorption spectrum of CN ( $B^2\Sigma^+ \leftarrow X^2\Sigma^+$ , 0-0 band), recorded 1 psec after application of 200-fsec, 248-nm photolysis pulse to ICN vapor.

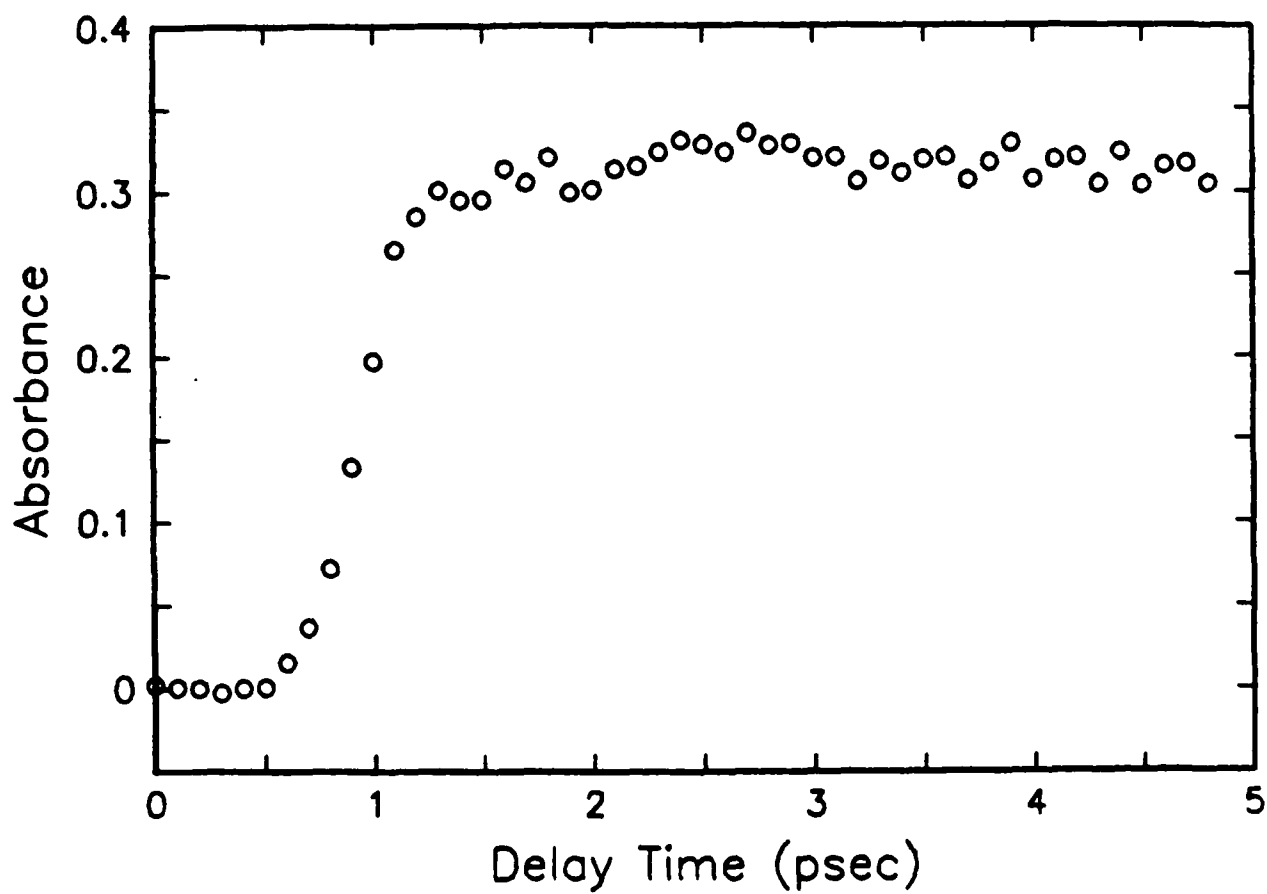


**Fig. 14** Growth of CN absorption spectrum following application of 200-fsec, 248-nm photolysis pulse to ICN vapor. Absorption measured at peak of the P-branch band head.

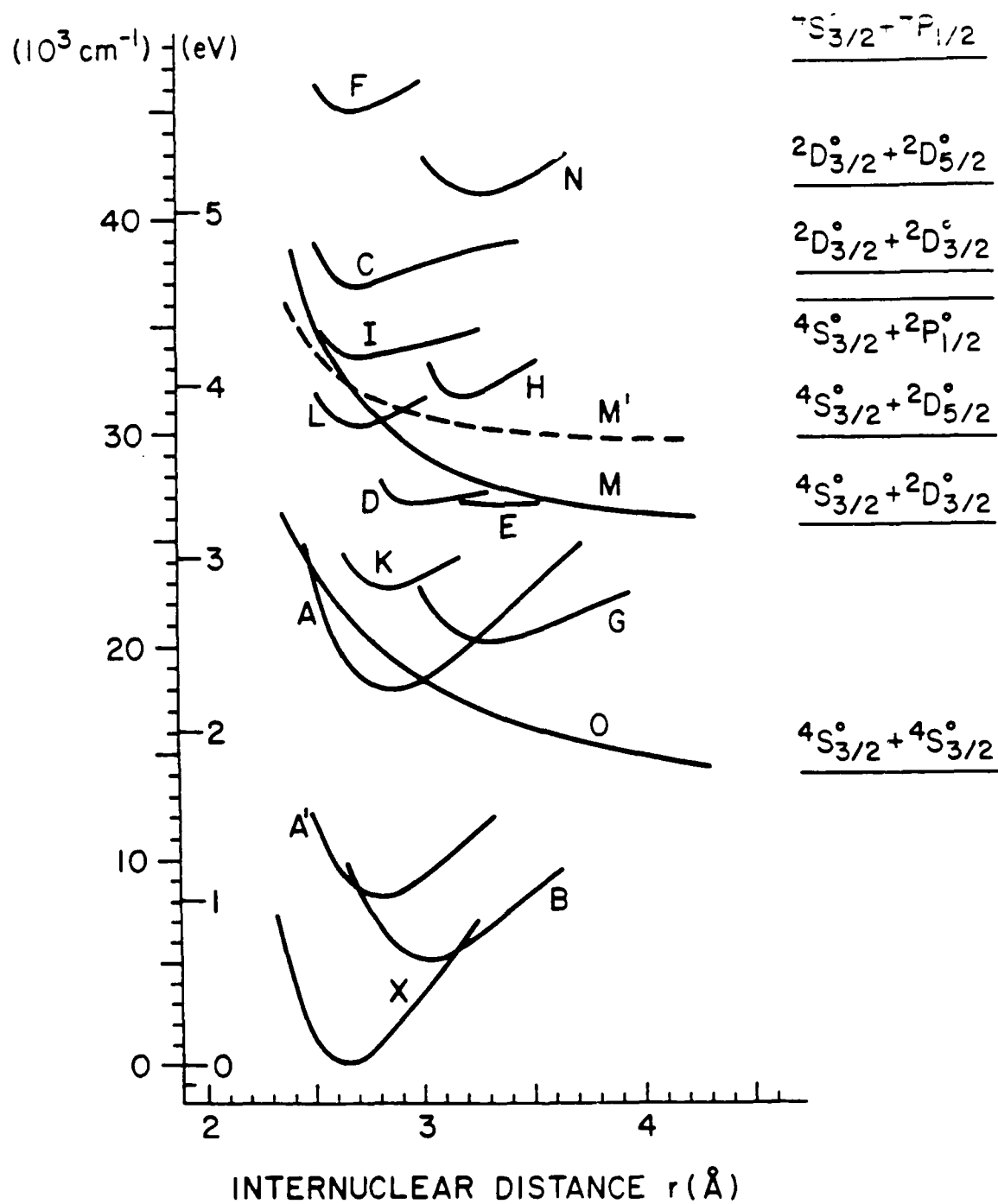


**Fig. 15** Electronic states of  $\text{Bi}_2$  as represented in G. Gerber and H.P. Broida, J. Chem. Phys. 64, 3423 (1976). The dashed curve (M') is schematically drawn as a result of our work (see text).

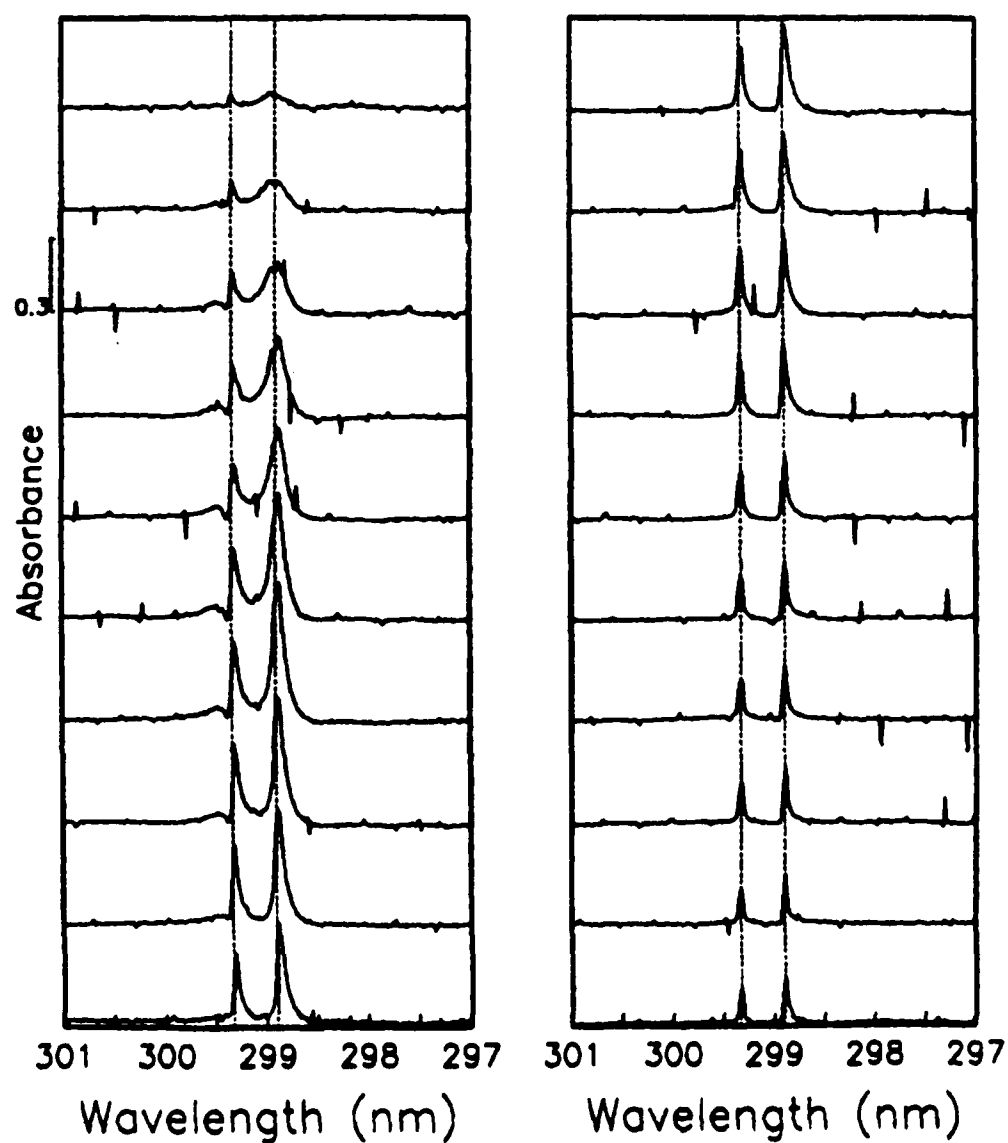


**Fig. 16** Transient absorption spectra taken in the vicinity of the Bi lines near 299.0, 299.3 nm. 100 fsec between successive spectra. Perpendicular pump, probe polarizations. Asymptotic line shapes not yet fully attained in this sequence.